

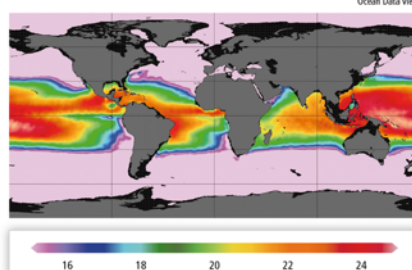
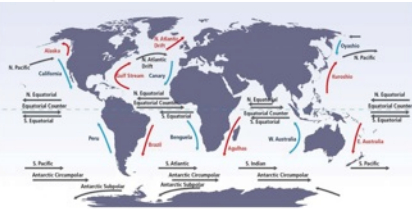
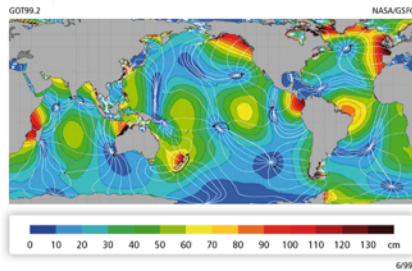
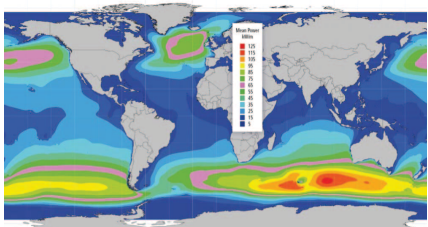
Quanta energia è possibile estrarre dai mari italiani?

G. Sannino

gianmaria.sannino@enea.it

Background – Global ocean energy distribution

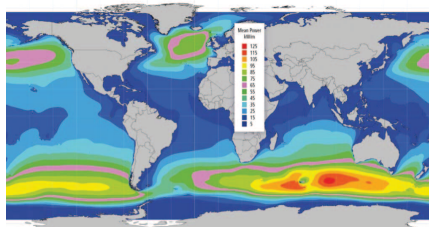
The RE resource in the ocean comes from six distinct sources, each with different origins and requiring different technologies for conversion.



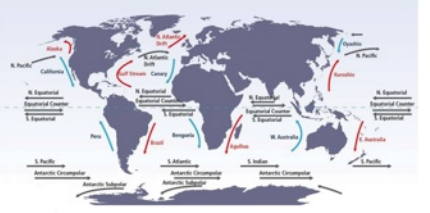
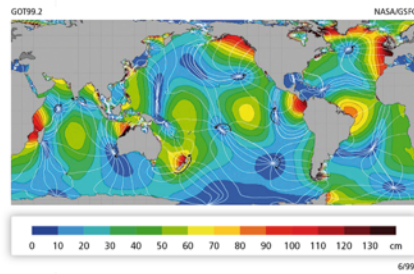
- **Waves:** derived from the transfer of the kinetic energy of the wind to the upper surface of the ocean.
- **Tidal Range (tidal rise and fall):** derived from the gravitational forces of the Earth-Moon-Sun system.
- **Tidal currents:** water flow resulting from the filling and emptying of coastal regions as a result of the tidal rise and fall.
- **Ocean Currents:** derived from wind-driven and thermohaline ocean circulation.
- **Ocean Thermal Energy Conversion (OTEC):** derived from temperature differences between solar energy stored as heat in upper ocean layers and colder seawater, generally below 1,000 m.
- **Salinity Gradients (osmotic power):** derived from salinity differences between fresh and ocean water at river mouths.

Background – Mediterranean energy

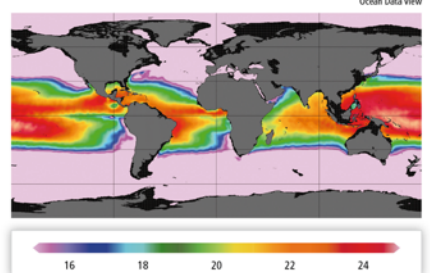
The RE resource in the ocean comes from six distinct sources, each with different origins and requiring different technologies for conversion.



- **Waves:** derived from the transfer of the kinetic energy of the wind to the upper surface of the ocean.



- **Tidal currents:** water flow resulting from the filling and emptying of coastal regions as a result of the tidal rise and fall.

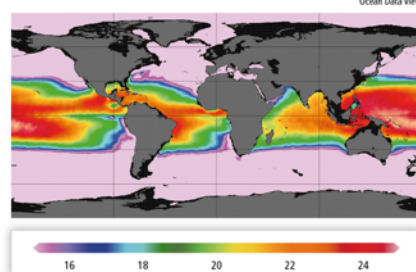
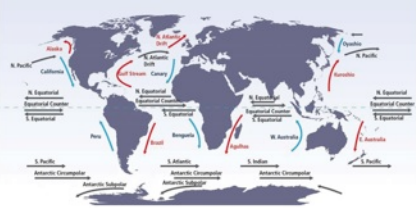
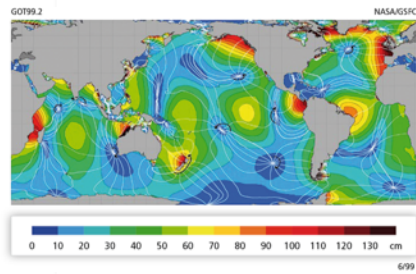
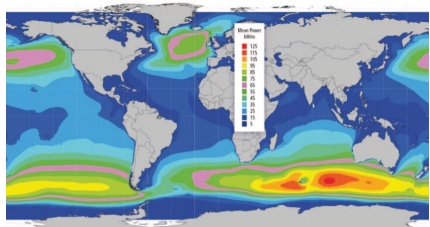


- **Ocean Currents:** derived from wind-driven and thermonaline ocean circulation.



Background – Mediterranean energy

The RE resource in the ocean comes from six distinct sources, each with different origins and requiring different technologies for conversion.



■ **Waves:** derived from the transfer of the kinetic energy of the wind to the upper surface of the ocean.

■ **Tidal Range (tidal rise and fall):** derived from the gravitational forces of the Earth-Moon-Sun system.

■ **Tidal currents:** water flow resulting from the filling and emptying of coastal regions as a result of the tidal rise and fall.

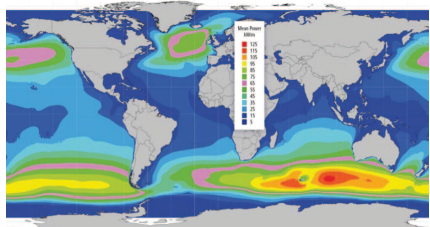
■ **Ocean Currents:** derived from wind-driven and thermohaline ocean circulation.

■ **Ocean Thermal Energy Conversion (OTEC):** derived from temperature differences between solar energy stored as heat in upper ocean layers and colder seawater, generally below 1,000 m.

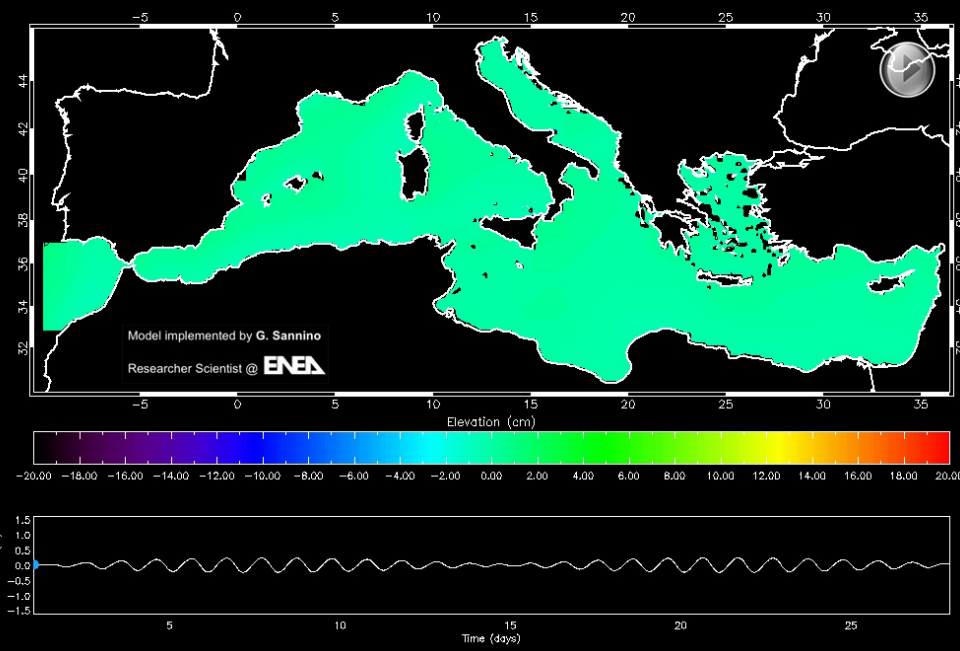
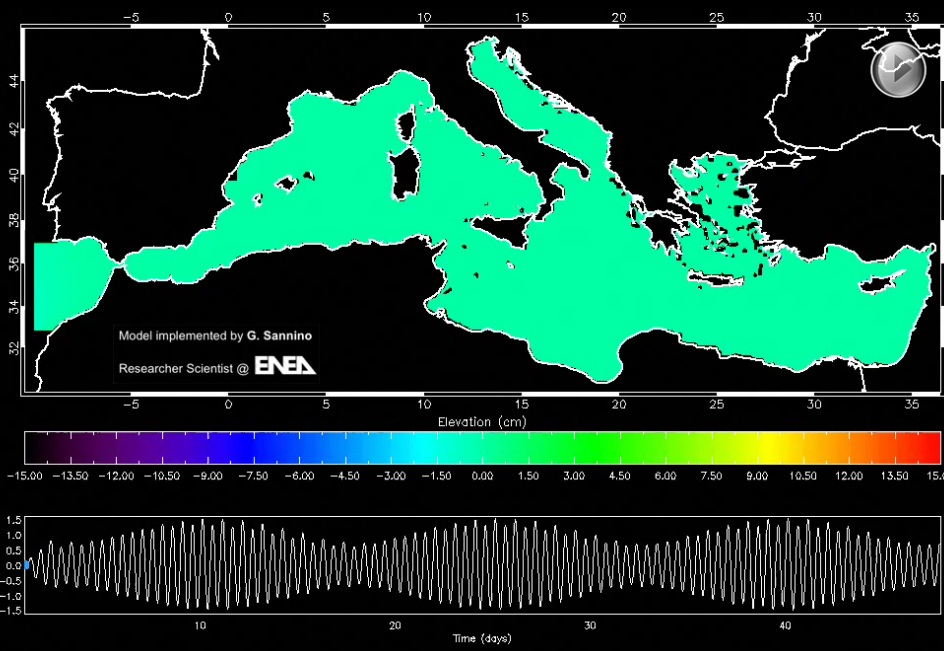
■ **Salinity Gradients (osmotic power):** derived from salinity differences between fresh and ocean water at river mouths.

Tidal energy assessment for the Mediterranean

Mediterranean and strait models



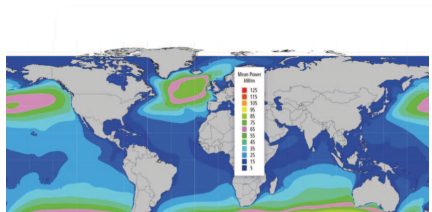
- **Tidal currents:** water flow resulting from the filling and emptying of coastal regions as a result of the tidal rise and fall.



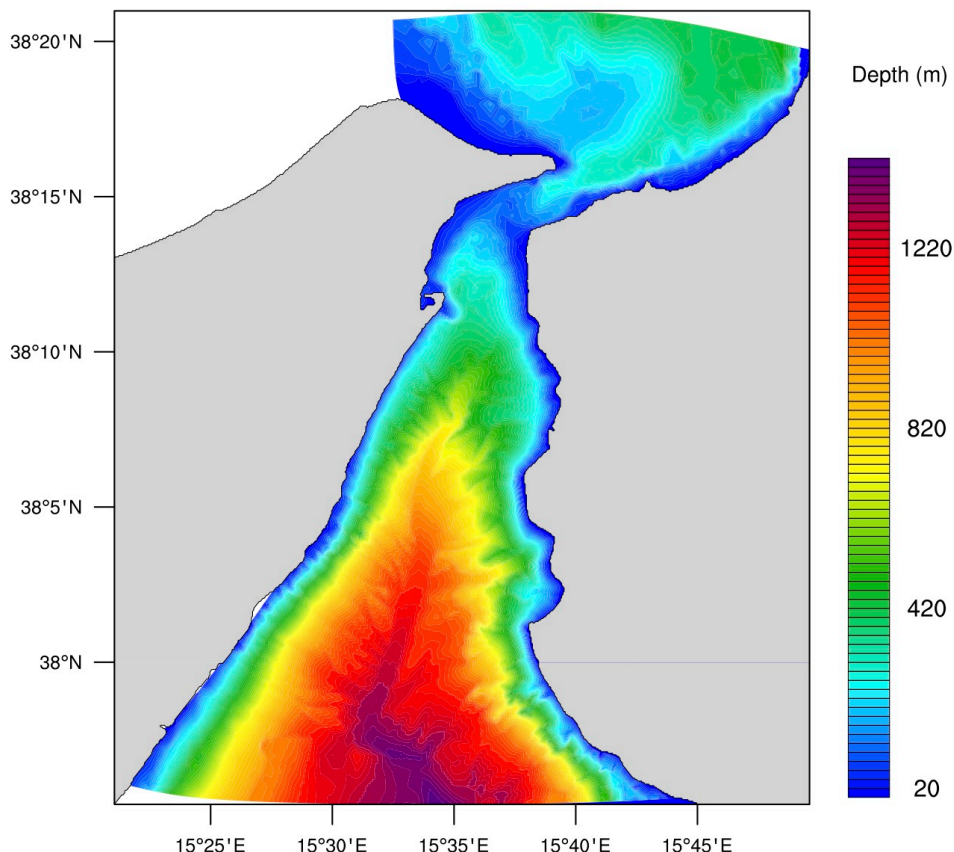
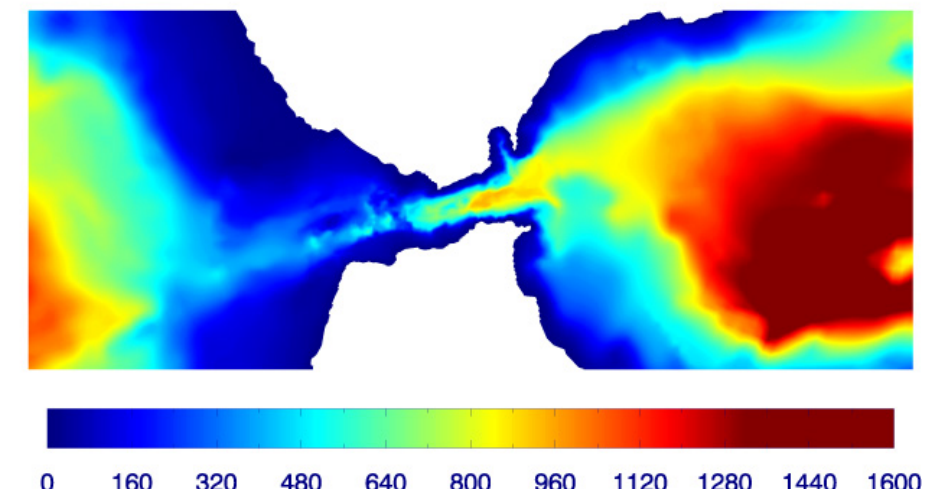
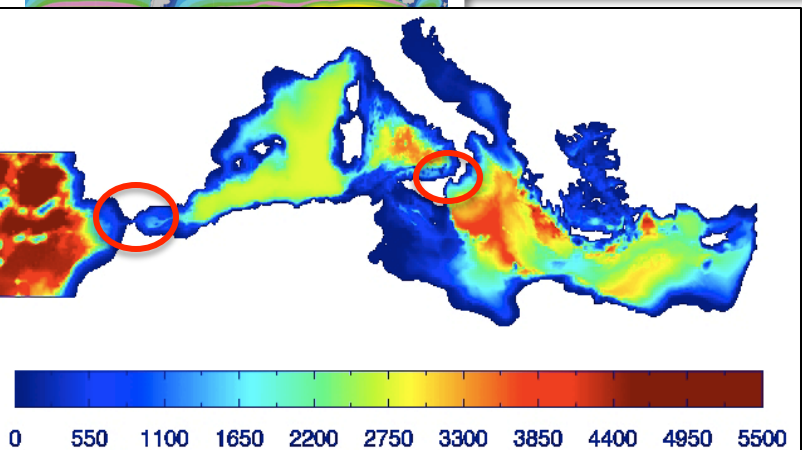
Tidal energy assessment for the Mediterranean

Mediterranean and strait models

Messina Strait topography

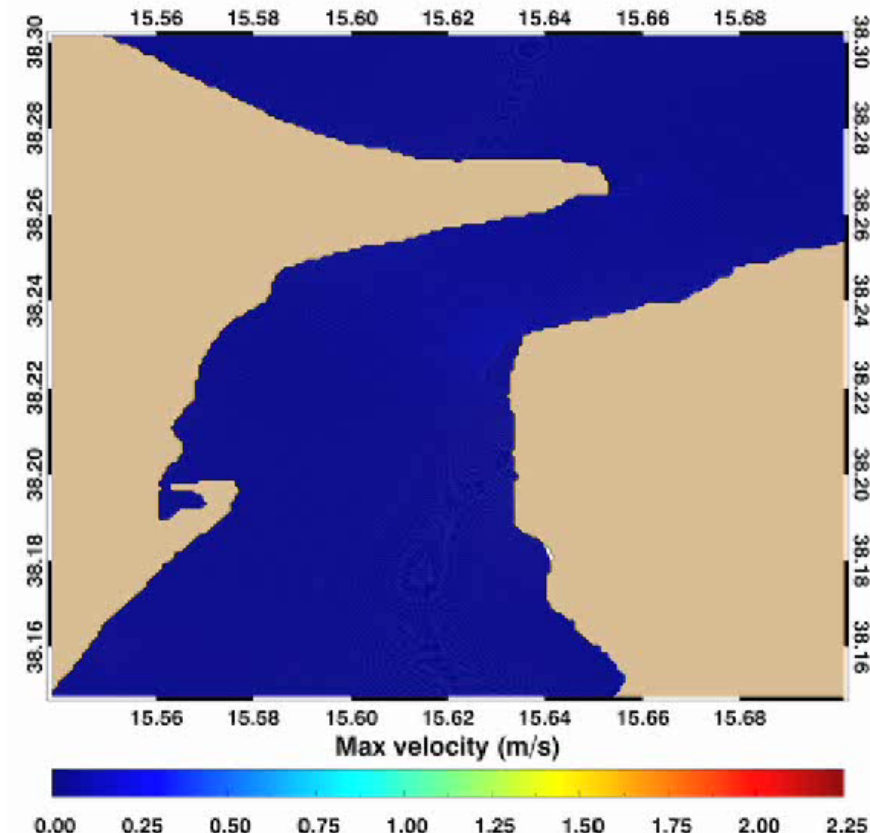
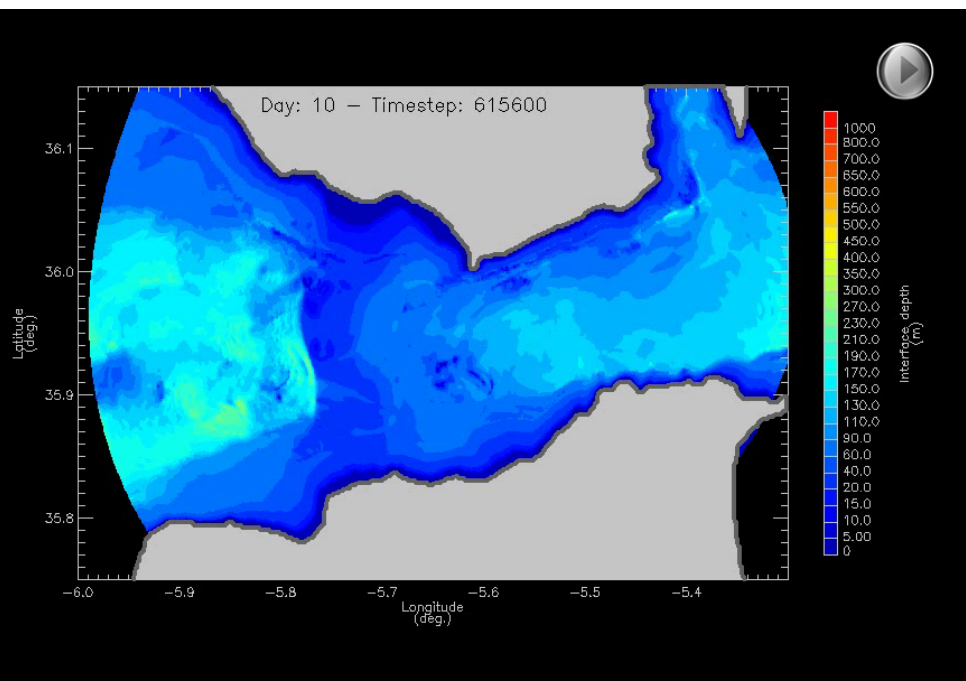


■ **Tidal currents:** water flow resulting from the filling and emptying of coastal regions as a result of the tidal rise and fall.



Tidal energy assessment for the Mediterranean

Gibraltar & Messina tidal models



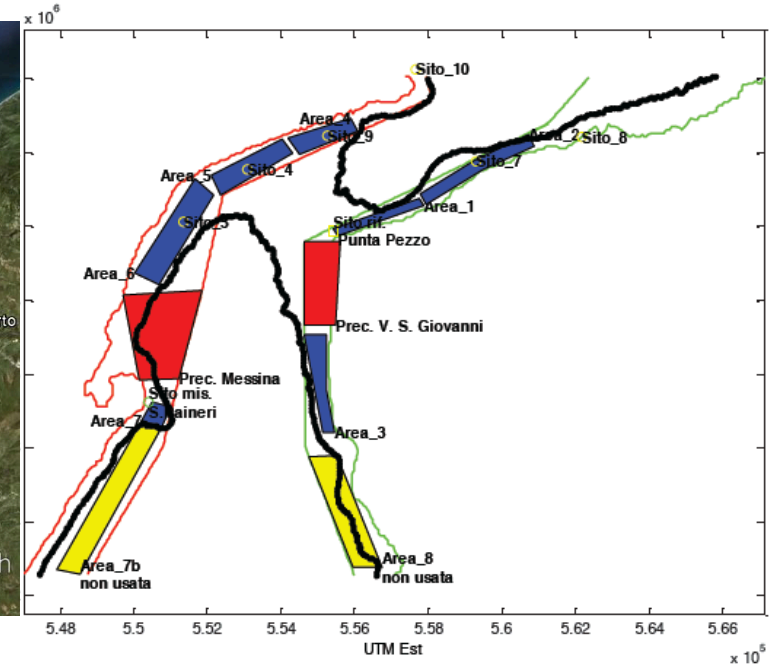
Model implemented: MITgcm

Resolution 1/200° x 1/200°

Tidal energy assessment for the Strait of Messina



Aree di installazione di ipotetiche fattorie energetiche marine



Aree di installazione prescelte (blu) con indicazione dei siti di misura e delle curve isobatimetriche a -20 m e a -150 m. In figura sono evidenziate aree di potenziale interesse non utilizzabili per limiti di navigabilità (rosso) o per difficoltà connesse alla batimetria (giallo).



ADAG
Aircraft
Design &
AeroFlightDynamics
Group



DIA
Dipartimento di Ingegneria Aerospaziale

UNIVERSITÀ DEGLI STUDI DI NAPOLI FEDERICO II

Prof. Domenico Corio

Tidal energy assessment for the Mediterranean

Gibraltar & Messina tidal models



UNIVERSITÀ DEGLI STUDI DI NAPOLI FEDERICO II



Il sistema **GEM**, anche denominato “aquilone del mare”, consiste in una struttura galleggiante che supporta due turbine idrauliche, eventualmente intubate in alcune configurazioni, per incrementare l’efficienza della conversione energetica. La struttura è collegata attraverso un cavo di ormeggio ad un ancoraggio al fondo marino, costituito anche da un semplice corpo morto. Il sistema può orientarsi autonomamente nella direzione della corrente, consentendo l’utilizzo del sistema anche in regimi di correnti alternanti

Tidal energy assessment for the Mediterranean

Gibraltar & Messina tidal models

Tabella 22. Produzioni fattorie – sistema GEM

<u>GEM</u>										
Località riferimento	Lat.	Lon.	Vmax (m/s)	Area impianto (km^2)	Densità (unità/km^2)	Numero unità	Potenza max unità (kW)	Potenza installata (kW)	Energia annua (MWh)	Ore equivalenti (h)
Punta Pezzo	38°14'00"N	15°38'00"E	2.95	0.5538		36	19	1001.1	19021.47	46240.5
<hr/>										
Località riferimento	Lat.	Lon.	Vmax (m/s)	Area impianto (km^2)	Densità (unità/km^2)	Numero unità	Potenza max unità (kW)	Potenza installata (kW)	Energia annua (MWh)	Ore equivalenti (h)
Adiacenze NW di T. Cavallo	38°15'00"N	15°40'40"E	1.60	1.1068		36	39	1001.1	39044.1	17959.4
Spiaggia tra Ganzirri e Torre Faro	38°15'24"N	15°37'54"E	2.17	0.8004		36	28	1001.1	28031.6	26144.6
Adiacenze di S. Agata	38°14'54"N	15°36'24"E	1.83	1.1819		36	42	1001.1	42047.5	28394.3
Adiacenze di Pace	38°14'09"N	15°35'12"E	1.61	2.0578		36	74	1001.1	74083.6	26420.6
<hr/>								Etot=	145159.5	MWh
					eta_wake=	0.712	Etot_wake=	103353.6	MWh	



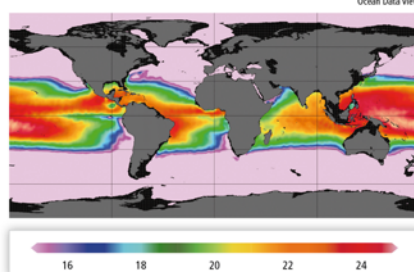
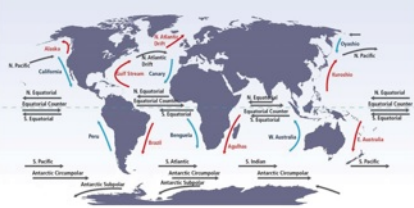
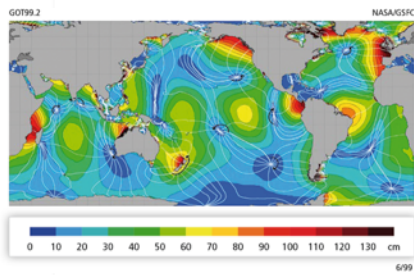
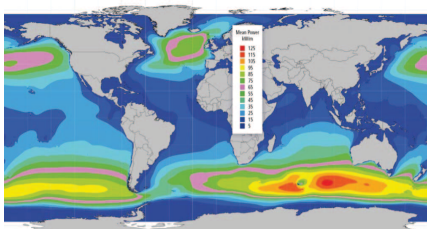
ADAG
Aircraft
Design &
AeroFlightDynamics
Group

UNIVERSITÀ DEGLI STUDI DI NAPOLI FEDERICO II

Prof. Domenico Corio

Background – Mediterranean energy

The RE resource in the ocean comes from six distinct sources, each with different origins and requiring different technologies for conversion.



■ **Waves:** derived from the transfer of the kinetic energy of the wind to the upper surface of the ocean.

■ **Tidal Range (tidal rise and fall):** derived from the gravitational forces of the Earth-Moon-Sun system.

■ **Tidal currents:** water flow resulting from the filling and emptying of coastal regions as a result of the tidal rise and fall.

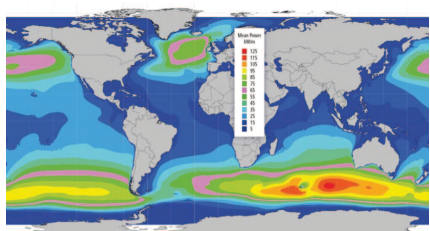
■ **Ocean Currents:** derived from wind-driven and thermohaline ocean circulation.

■ **Ocean Thermal Energy Conversion (OTEC):** derived from temperature differences between solar energy stored as heat in upper ocean layers and colder seawater, generally below 1,000 m.

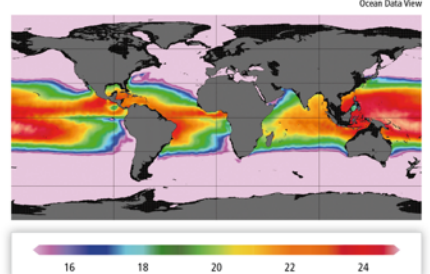
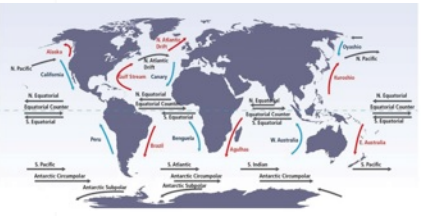
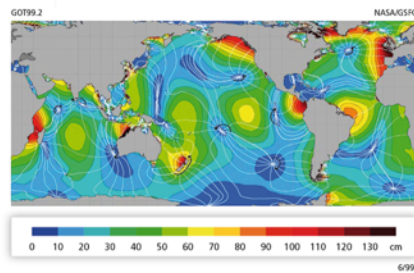
■ **Salinity Gradients (osmotic power):** derived from salinity differences between fresh and ocean water at river mouths.

Background – Mediterranean energy

The RE resource in the ocean comes from six distinct sources, each with different origins and requiring different technologies for conversion.

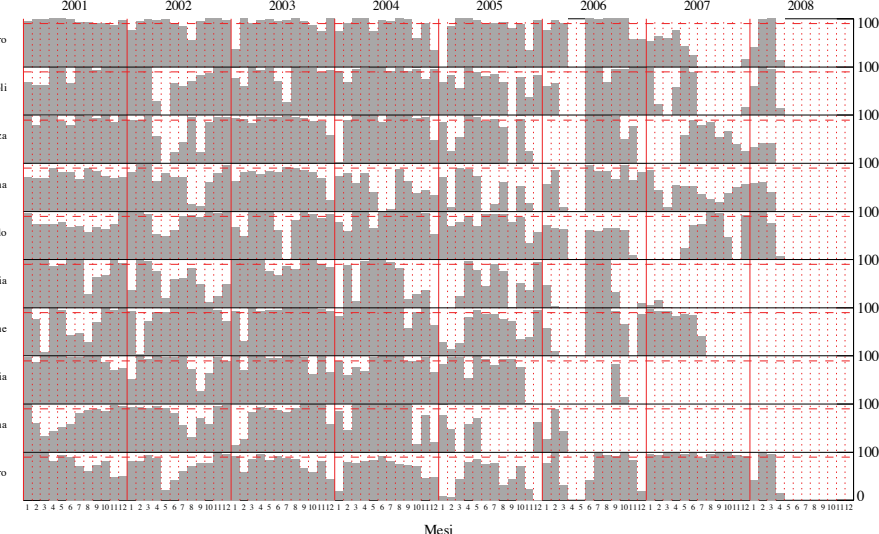


- **Waves:** derived from the transfer of the kinetic energy of the wind to the upper surface of the ocean.



Wave energy assessment along the Italian coasts

Traditional approach: using the Italian Wave measuring Network (Rete Ondametrica Nazionale, RON) managed by Institute for Environmental Protection and Research (ISPRA)



Buoy	First Record	Last Record	3hr Records after 1/1/2001	Expected 3hr records	Efficiency (%)
Alghero	01/07/1989	05/04/2008	15283	21210	72.1
Catania	01/07/1989	05/10/2006	12549	16827	80.2
Crotone	01/07/1989	15/07/2007	14962	19093	78.4
La Spezia	01/07/1989	31/03/2007	10952	18240	60.0
Mazara del Vallo	01/07/1989	04/04/2008	15323	21207	72.3
Monopoli	01/07/1989	05/04/2008	15641	21209	73.7
Ortona	01/07/1989	24/03/2008	12786	21113	60.6
Ponza	01/07/1989	31/03/2008	14479	21169	68.4
Cetraro	28/02/1999	05/04/2008	16630	21209	78.4
Ancona	10/03/1999	31/05/2006	10212	15812	64.6
Capo Comino	01/01/2004	12/09/2005	3813	5664	67.3
Capo Gallo	01/01/2004	31/03/2008	9001	12408	72.5
Capo Linaro	02/01/2004	12/09/2006	5441	7872	69.1
Punta della Maestra	02/01/2004	24/11/2004	2616	7872	62.8
Cagliari	06/02/2007	02/03/2008	1986	3120	63.7



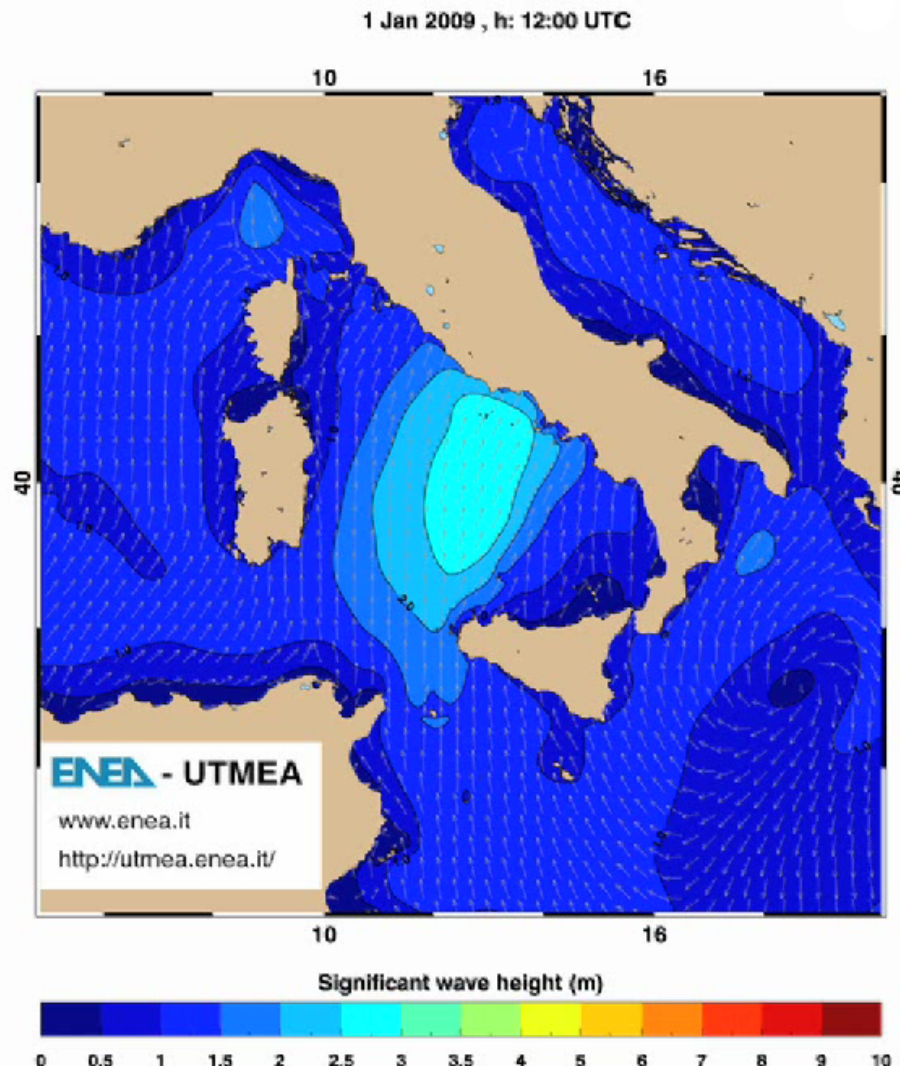
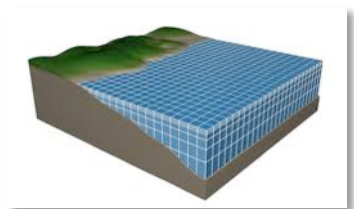
ISPRA
Istituto Superiore per la Protezione
e la Ricerca Ambientale

Wave energy assessment along the Italian coasts

Our approach: using a relatively high resolution wave model

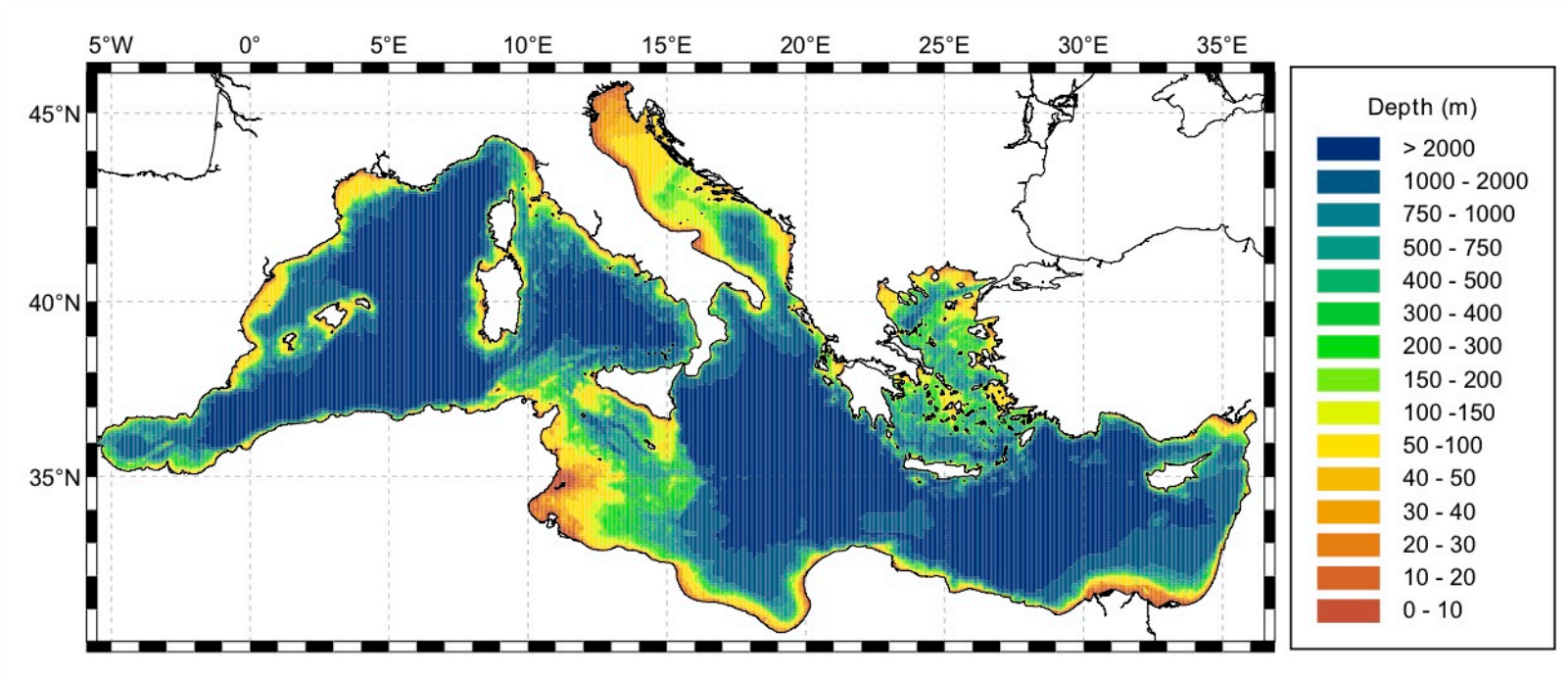


www.cresco.enea.it



Numerical modeling approach

Numerical Wave model description



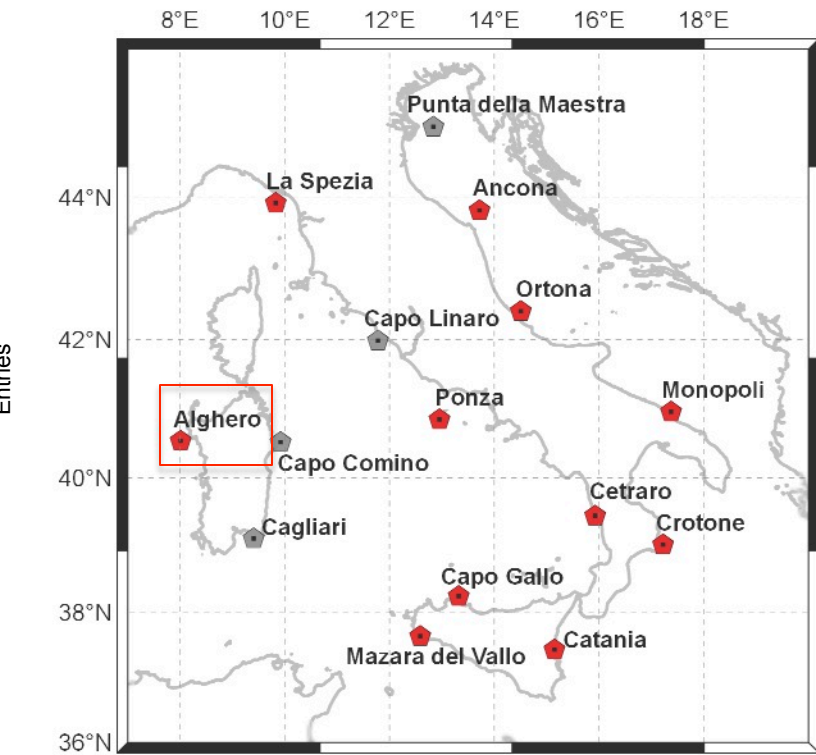
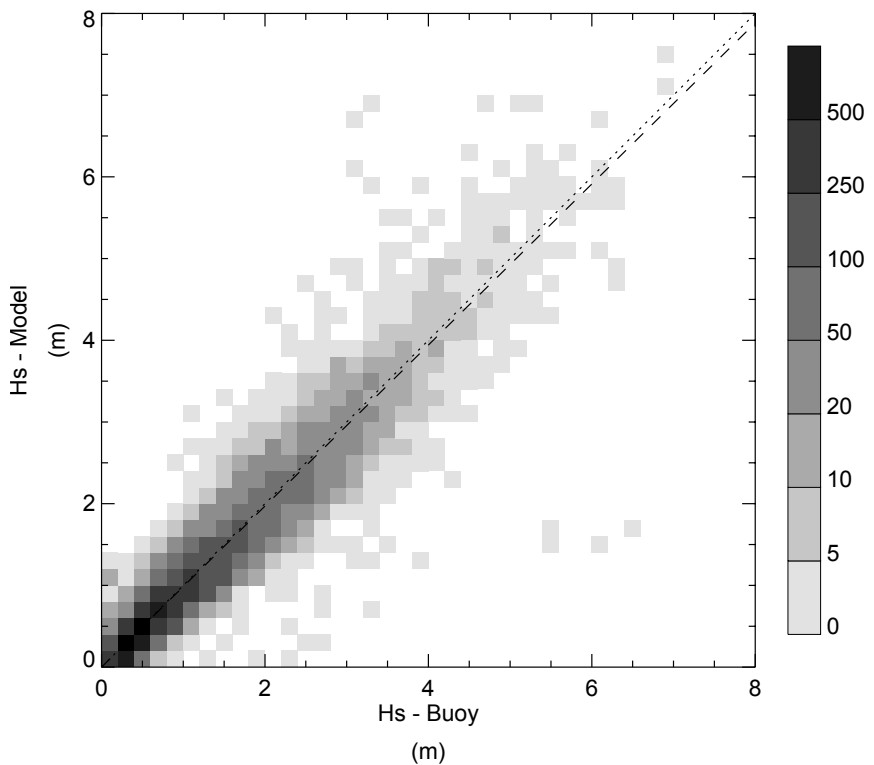
Model implemented: WAM (*Wave prediction Model*)

Resolution 1/16° x 1/16° (about 7Km)

ECMWF (European Centre for Medium range Weather Forecast) wind field data (analysis)

Numerical wave model validation (Hs)

Numerical Wave model vs buoy: ALGHERO

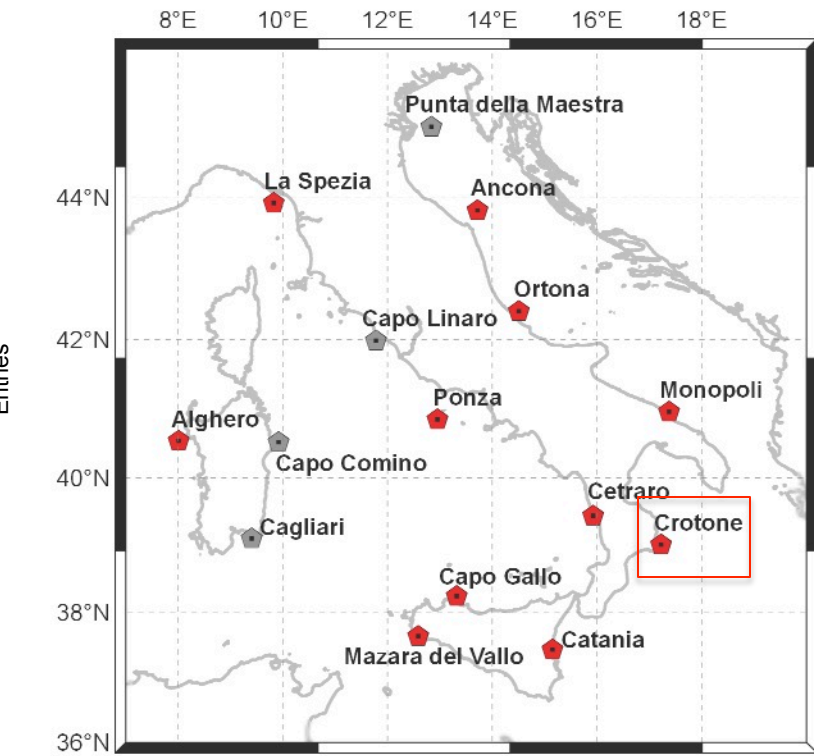
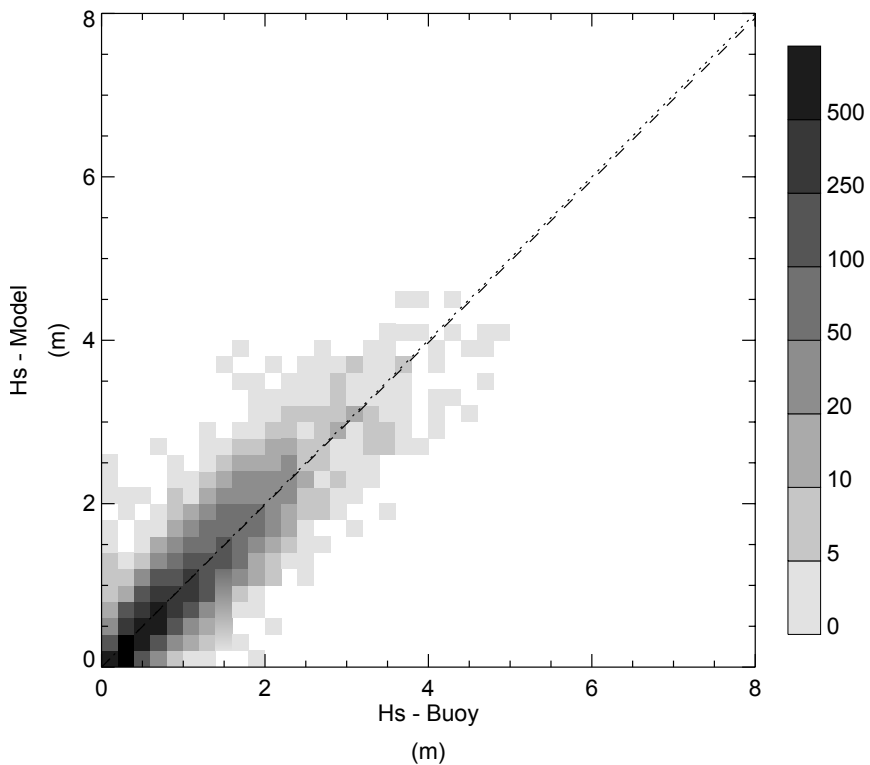


Correlation between buoy and model H_s at **Alghero**. Dashed line is the best fit line between model and buoy data points.

Period considered 2001-2010

Numerical wave model validation (Hs)

Numerical Wave model vs buoy: CROTONE

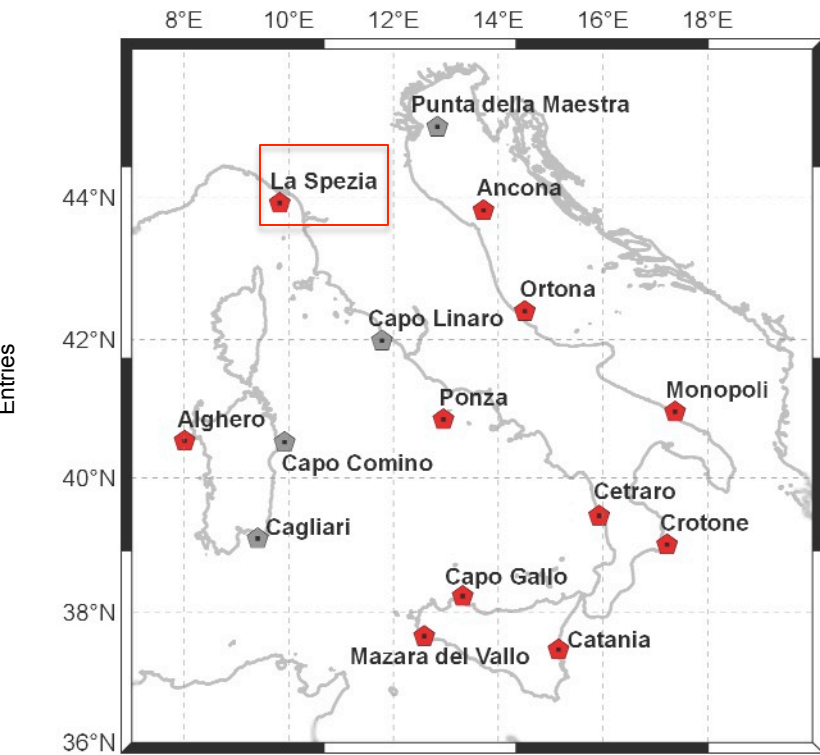
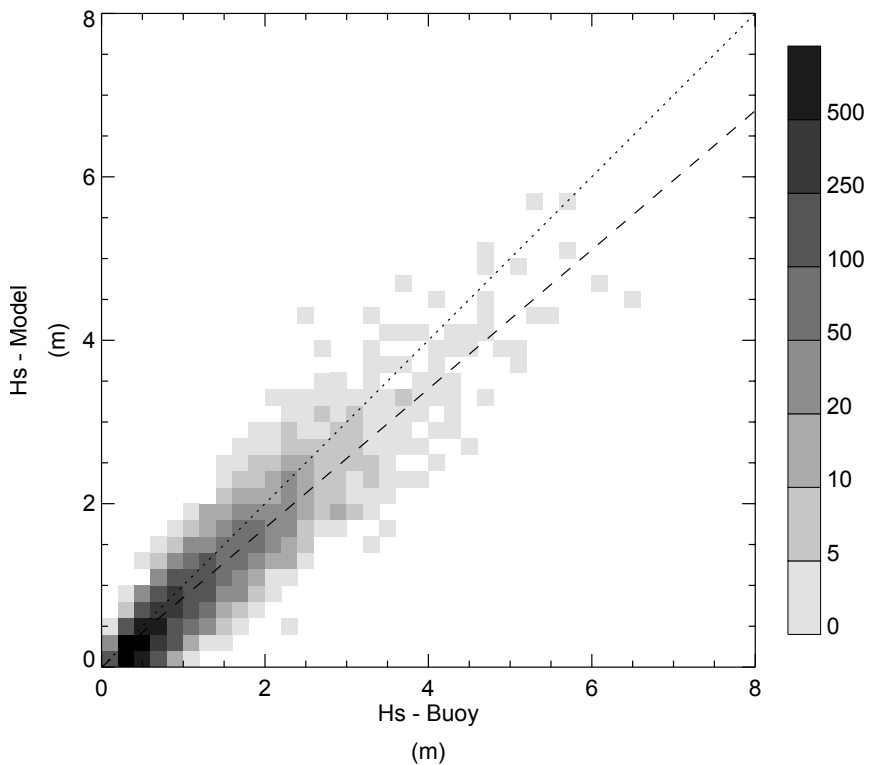


Correlation between buoy and model H_s at **Crotone**. Dashed line is the best fit line between model and buoy data points.

Period considered 2001-2010

Numerical wave model validation (Hs)

Numerical Wave model vs buoy: LA SPEZIA

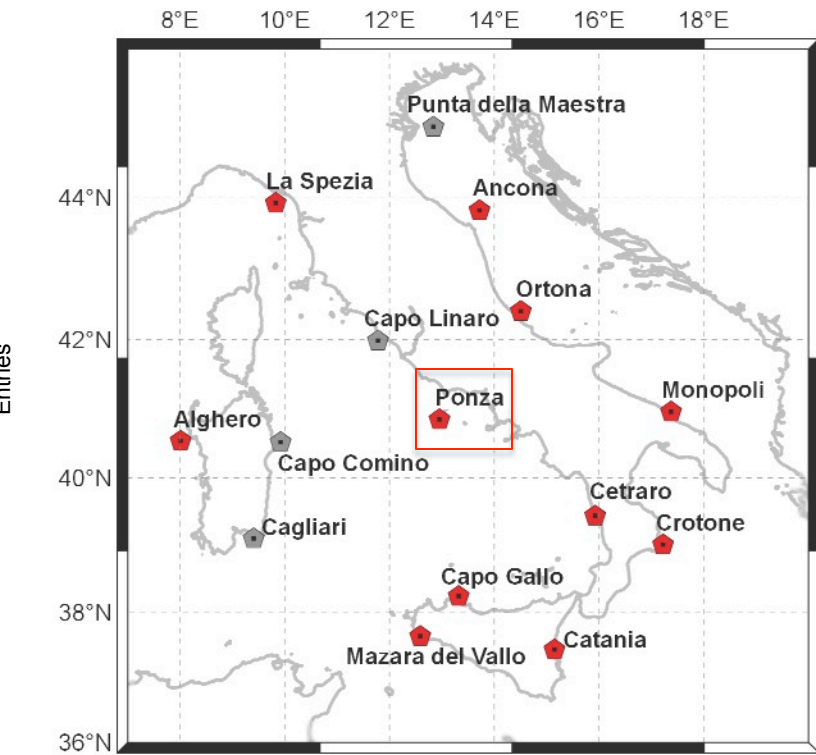
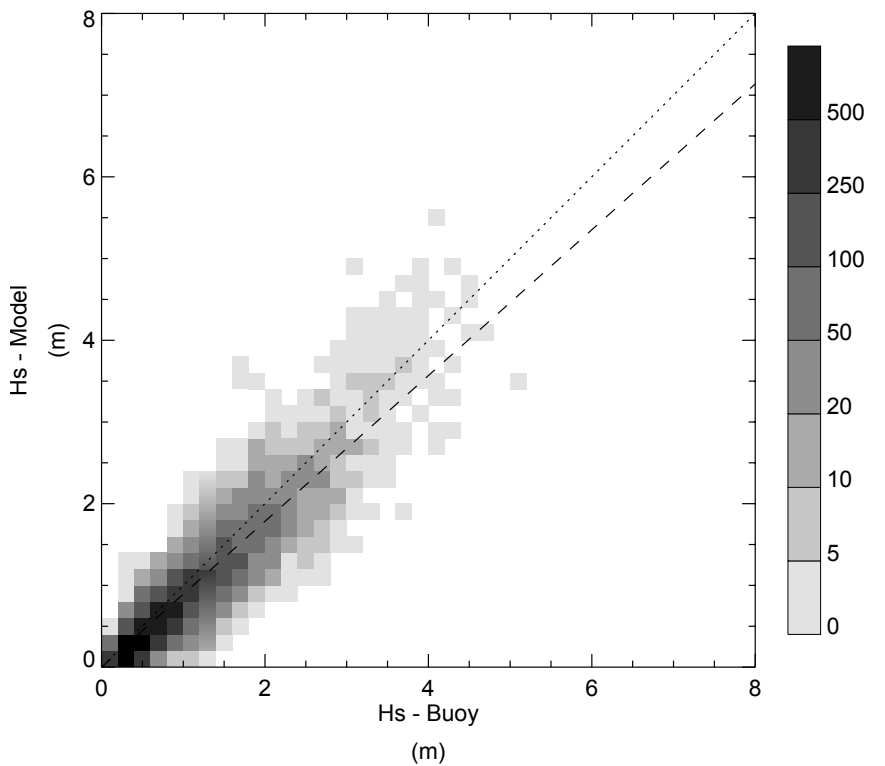


Correlation between buoy and model H_s at **La Spezia**. Dashed line is the best fit line between model and buoy data points.

Period considered 2001-2010

Numerical wave model validation (Hs)

Numerical Wave model vs buoy: PONZA

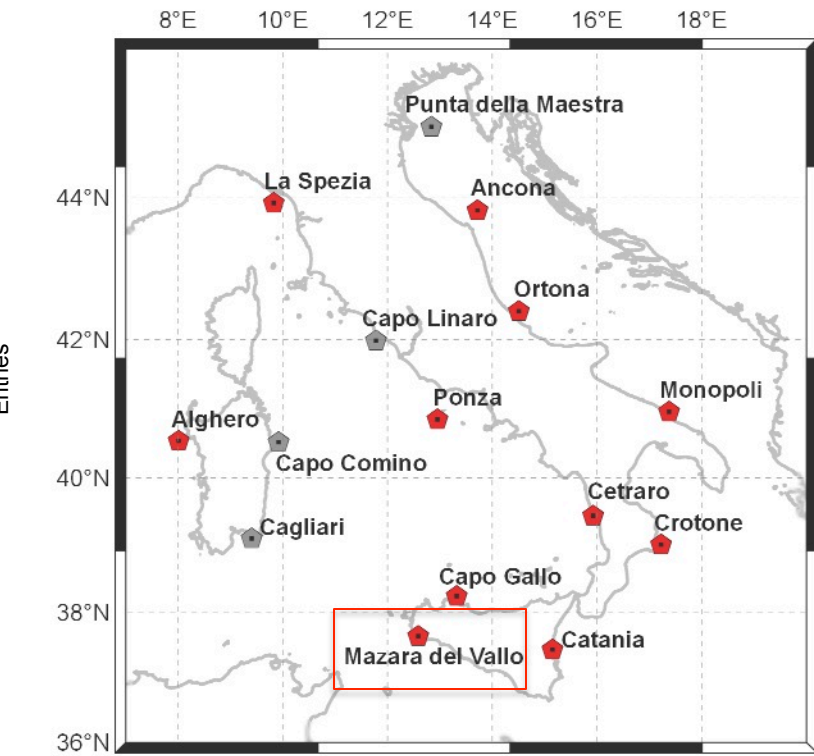
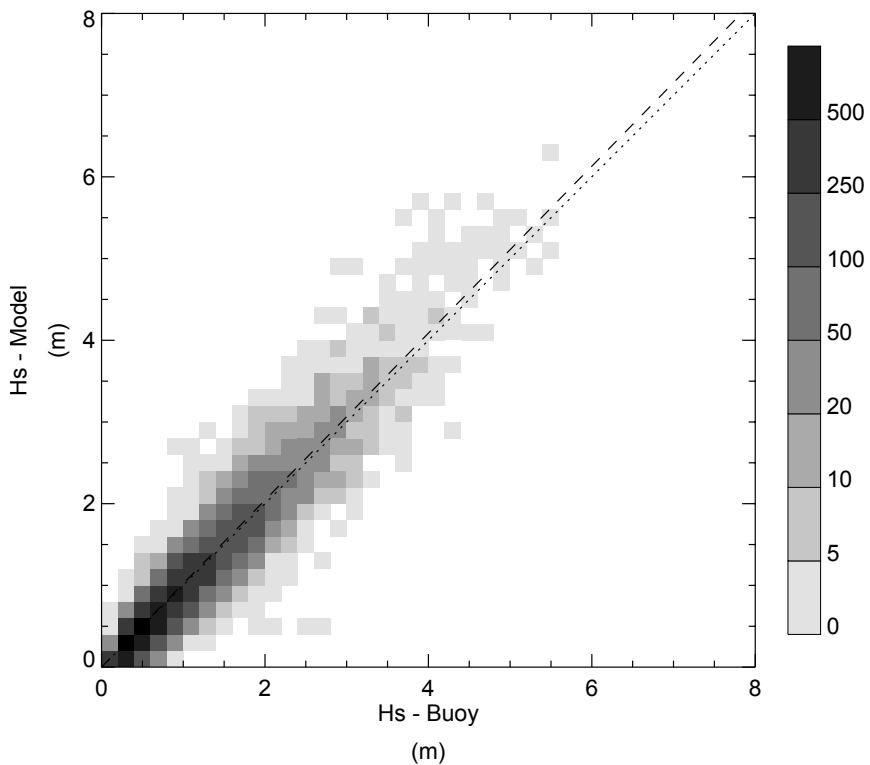


Correlation between buoy and model H_s at **Ponza**. Dashed line is the best fit line between model and buoy data points.

Period considered 2001-2010

Numerical wave model validation (Hs)

Numerical Wave model vs buoy



Correlation between buoy and model H_s at **Mazara del Vallo**. Dashed line is the best fit line between model and buoy data points.

Period considered 2001-2010

Numerical wave model validation (H_s)

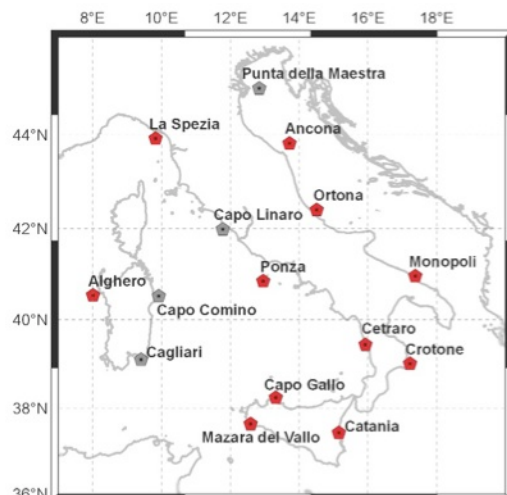
Numerical Wave model vs buoy: statistics

$$bias = \frac{1}{n} \sum_{i=1}^n (y_i - x_i),$$

$$rmse = \sqrt{\frac{1}{n-1} \sum_{i=1}^n (y_i - x_i)^2},$$

$$si = \frac{rmse}{\frac{1}{n} \sum_{i=1}^n y_i},$$

$$slope = \frac{\sum_{i=1}^n x_i y_i}{\sum_{i=1}^n x_i x_i}.$$



Buoy	Bias (m)	Rmse (m)	Slope	Si
Alghero	-0.005	0.311	0.985	0.278
Ancona	-0.214	0.361	0.725	0.477
Catania	-0.178	0.308	0.747	0.501
Crotone	0.004	0.276	0.993	0.374
La Spezia	-0.143	0.283	0.851	0.354
Mazara del Vallo	0.013	0.257	1.022	0.253
Ortona	-0.150	0.284	0.753	0.460
Ponza	-0.103	0.273	0.892	0.328
Monopoli	-0.124	0.307	0.836	0.427
Cetraro	-0.070	0.241	0.897	0.341
Capo Gallo	0.019	0.255	1.040	0.339

Statistics of buoy and model significant wave height (H_s) comparison.

Period considered 2001-2010

Numerical wave model validation (Direction)

Numerical Wave model vs buoy: statistics

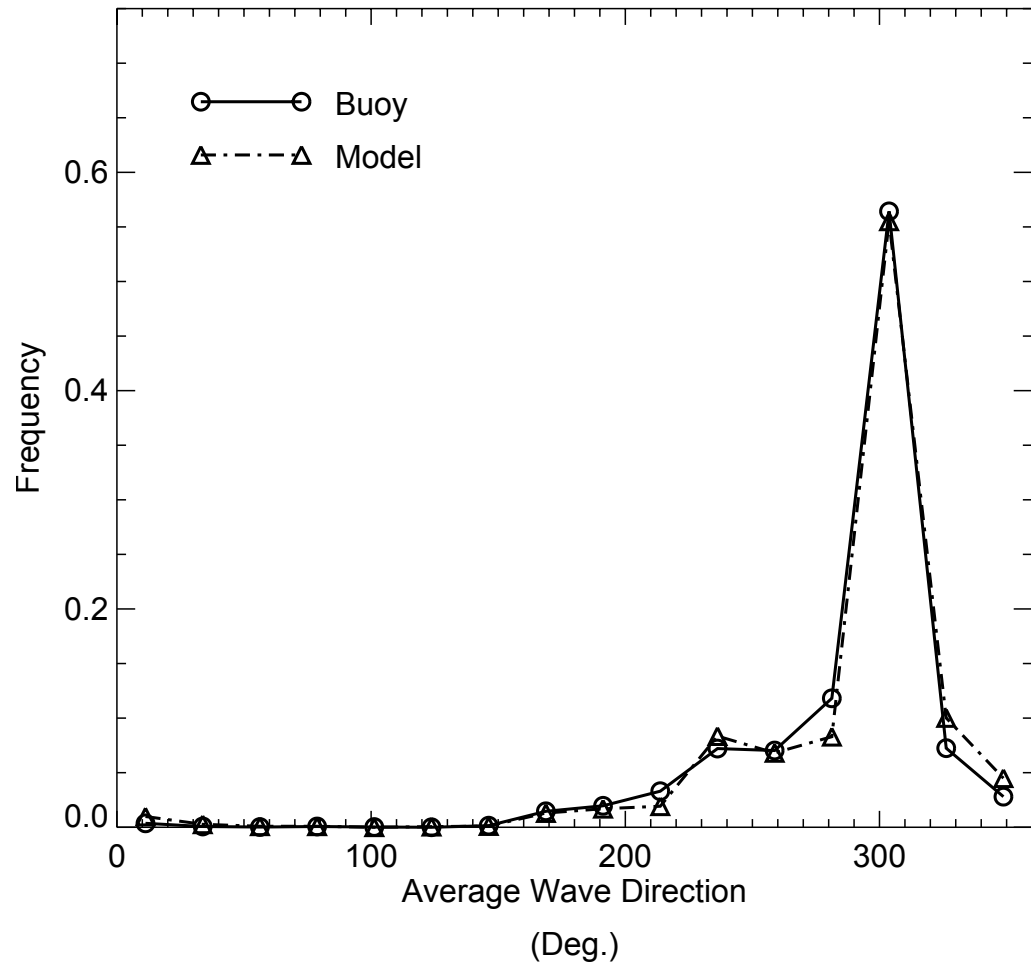
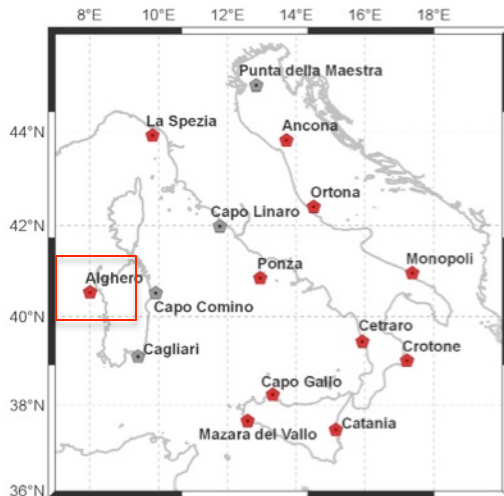
$$\bar{S} = \frac{1}{n} \sum_{i=1}^n \sin(y_i - x_i),$$

$$\bar{C} = \frac{1}{n} \sum_{i=1}^n \cos(y_i - x_i),$$

$$\bar{R} = (\bar{C}^2 + \bar{S}^2)^{\frac{1}{2}},$$

$$bias^\circ = \arctan(\bar{S}/\bar{C}),$$

$$var^\circ = (1 - \bar{R}).$$



Frequency distribution of model and buoy average wave direction at **Alghero**. Only records with $H_s > 1$ m are considered. Incoming wave direction is indicated as degrees in clockwise direction from the north.

Period considered 2001-2010

Numerical wave model validation (Direction)

Numerical Wave model vs buoy: statistics

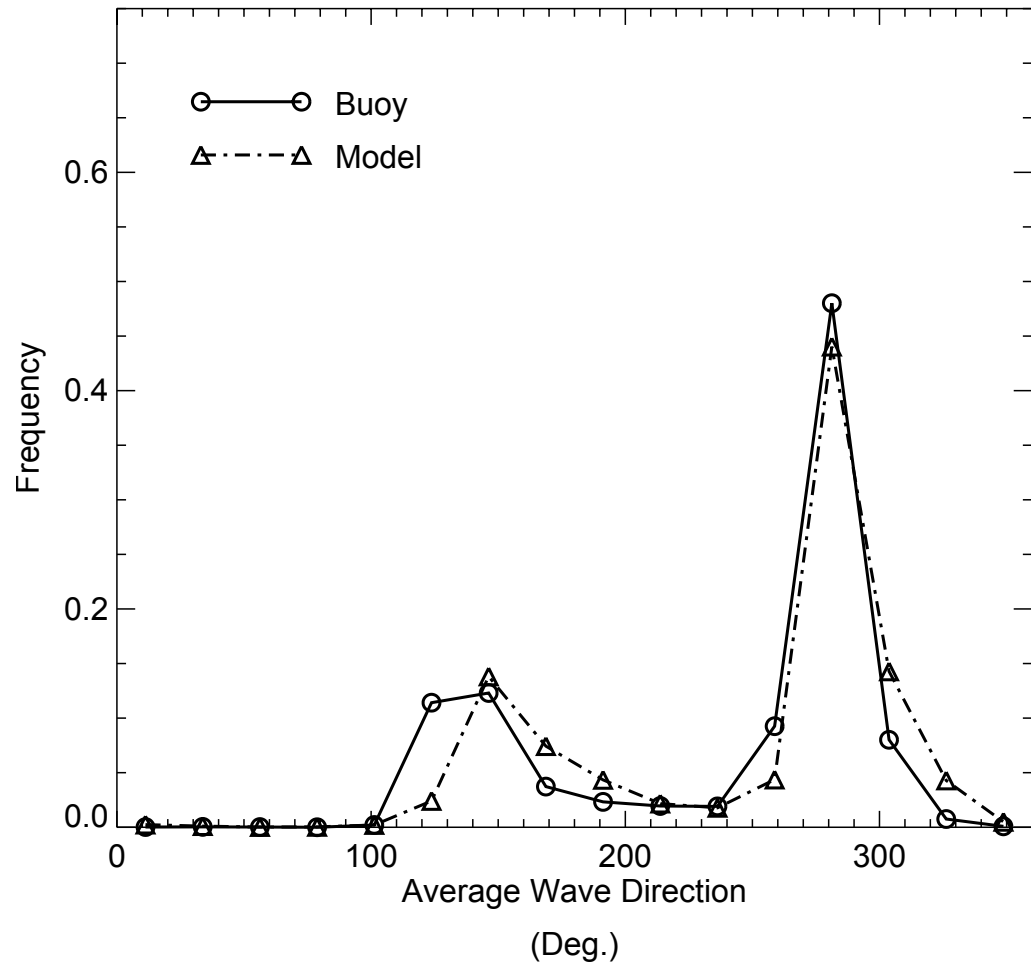
$$\bar{S} = \frac{1}{n} \sum_{i=1}^n \sin(y_i - x_i),$$

$$\bar{C} = \frac{1}{n} \sum_{i=1}^n \cos(y_i - x_i),$$

$$\bar{R} = (\bar{C}^2 + \bar{S}^2)^{\frac{1}{2}},$$

$$bias^\circ = \arctan(\bar{S}/\bar{C}),$$

$$var^\circ = (1 - \bar{R}).$$



Frequency distribution of model and buoy average wave direction at **Mazara del Vallo**. Only records with $H_s > 1$ m are considered.

Incoming wave direction is indicated as degrees in clockwise direction from the north.

Period considered 2001-2010

Numerical wave model validation (Direction)

Numerical Wave model vs buoy: statistics

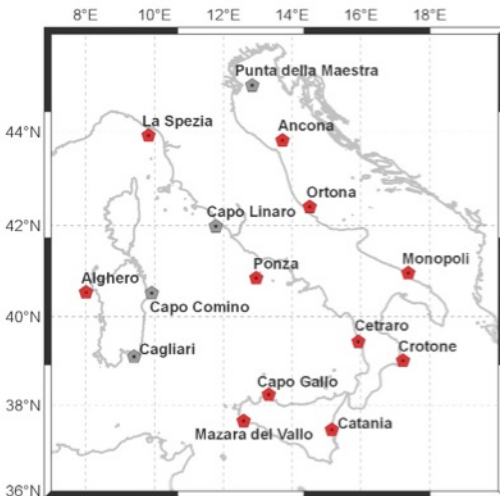
$$\bar{S} = \frac{1}{n} \sum_{i=1}^n \sin(y_i - x_i),$$

$$\bar{C} = \frac{1}{n} \sum_{i=1}^n \cos(y_i - x_i),$$

$$\bar{R} = (\bar{C}^2 + \bar{S}^2)^{\frac{1}{2}},$$

$$bias^\circ = \arctan(\bar{S}/\bar{C}),$$

$$var^\circ = (1 - \bar{R}).$$



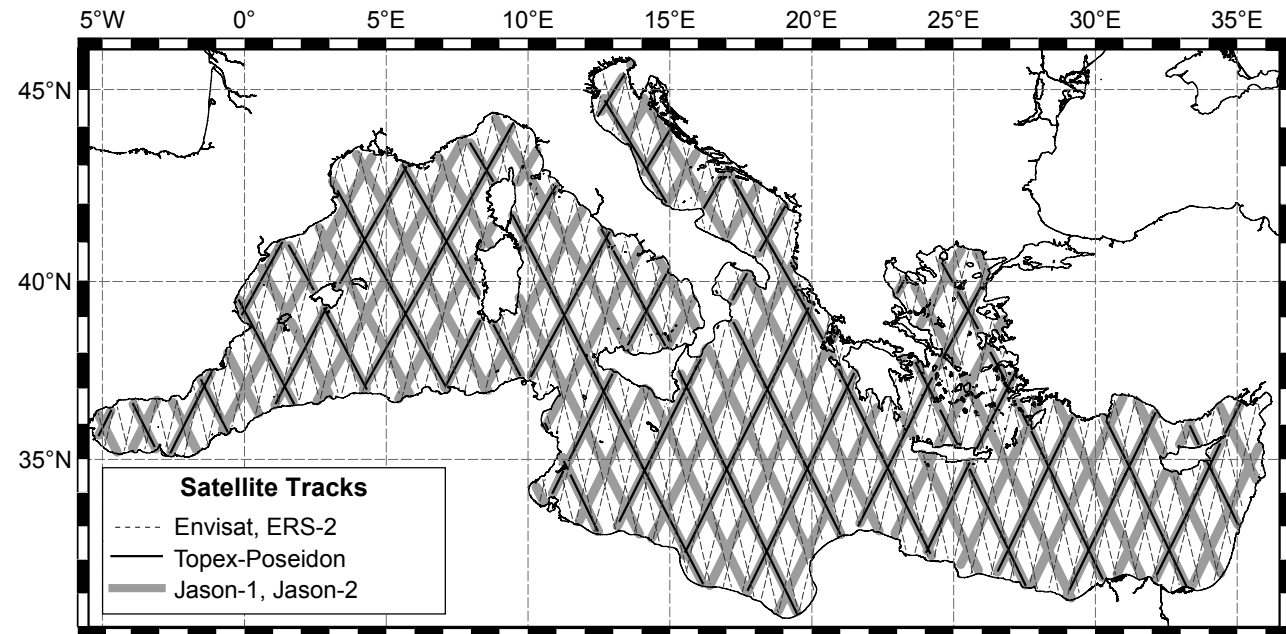
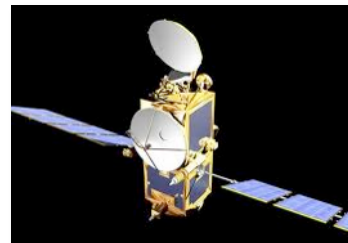
Buoy	$Bias^\circ$ (Deg.)	Var°
Alghero	4.51	0.036
Ancona	9.41	0.230
Catania	14.81	0.053
Crotone	8.09	0.085
La Spezia	2.94	0.056
Mazara del Vallo	11.00	0.057
Ortona	13.48	0.101
Ponza	8.76	0.116
Monopoli	5.00	0.121
Cetraro	6.39	0.063
Capo Gallo	-5.21	0.026

Circular statistics of buoy and model wave average spectral direction comparison.

Period considered 2001-2010

Numerical wave model validation

Numerical Wave model vs satellite altimeter



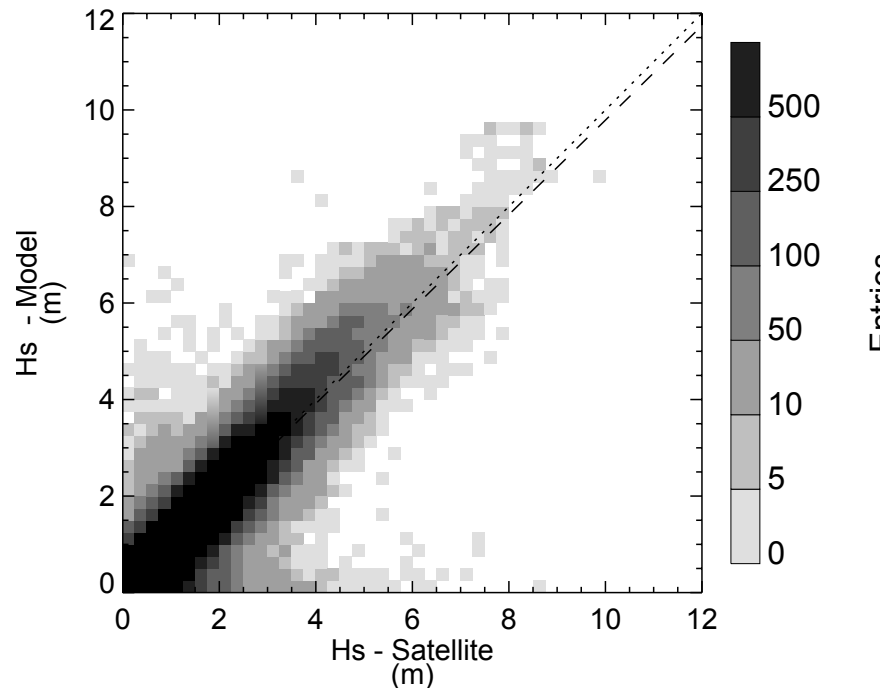
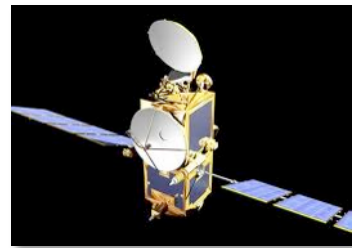
Ground tracks of satellites considered in model validation. Thick grey lines identify **Jason-1** and **Jason-2** tracks. Black lines partially overlying the grey ones symbolize **Topex-Poseidon** tracks while thin dashed lines represent **Envisat** and **ERS-2** tracks

Satellite	Repeat Cycle (days)	Used Period	Track Separation at Equator (km)
Topex-Poseidon	10	Jan. 2001 - Oct. 2005	315
Jason-1	10	Jan. 2002 - Dec. 2010	315
Jason-2	10	Jun. 2008 - Dec. 2010	315
Envisat	35	Oct. 2002 - Oct. 2010	80
ERS-2	35	Jan. 2001 - Dec. 2006 Jan. 2008 - Dec. 2010	80

Characteristics of satellites used in this study.

Numerical wave model validation

Numerical Wave model vs satellite altimeter



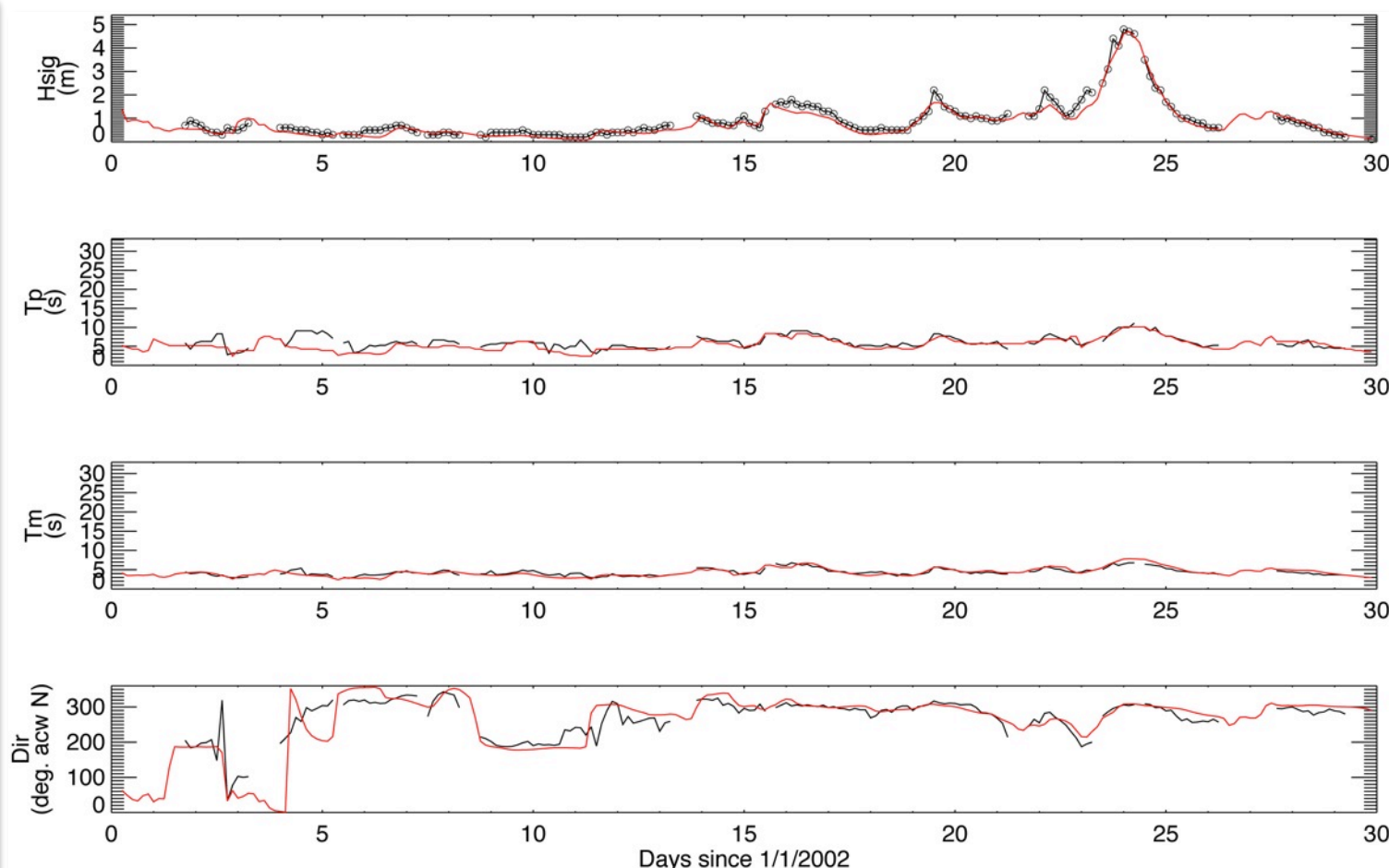
Scatter plot of model vs. Jason-1 H_s for the entire Mediterranean. Value pairs are grouped in 0.25 m wide bins, corresponding areas are painted according to the number of entries in each bin. Dashed line is the best fit line between model and satellite data points.

Satellite	Samples	Bias (m)	Rmse (m)	Slope	Si
Topex-Poseidon	457,000	-0.128	0.331	0.912	0.279
Jason-1	910,133	-0.028	0.362	0.979	0.304
Jason-2	242,766	0.024	0.366	1.018	0.303
Envisat	695,768	-0.141	0.385	0.921	0.310
ERS-2	363,336	-0.011	0.426	0.962	0.400

Statistics of satellite and model significant wave height H_s comparison for the entire Mediterranean.

Numerical wave model validation

Numerical Wave model vs buoy: ALGHERO



Andamento delle altezze significative (H_s) in metri della simulazione SIM_ECMWF rispetto ai dati relativi alla boa di Alghero.

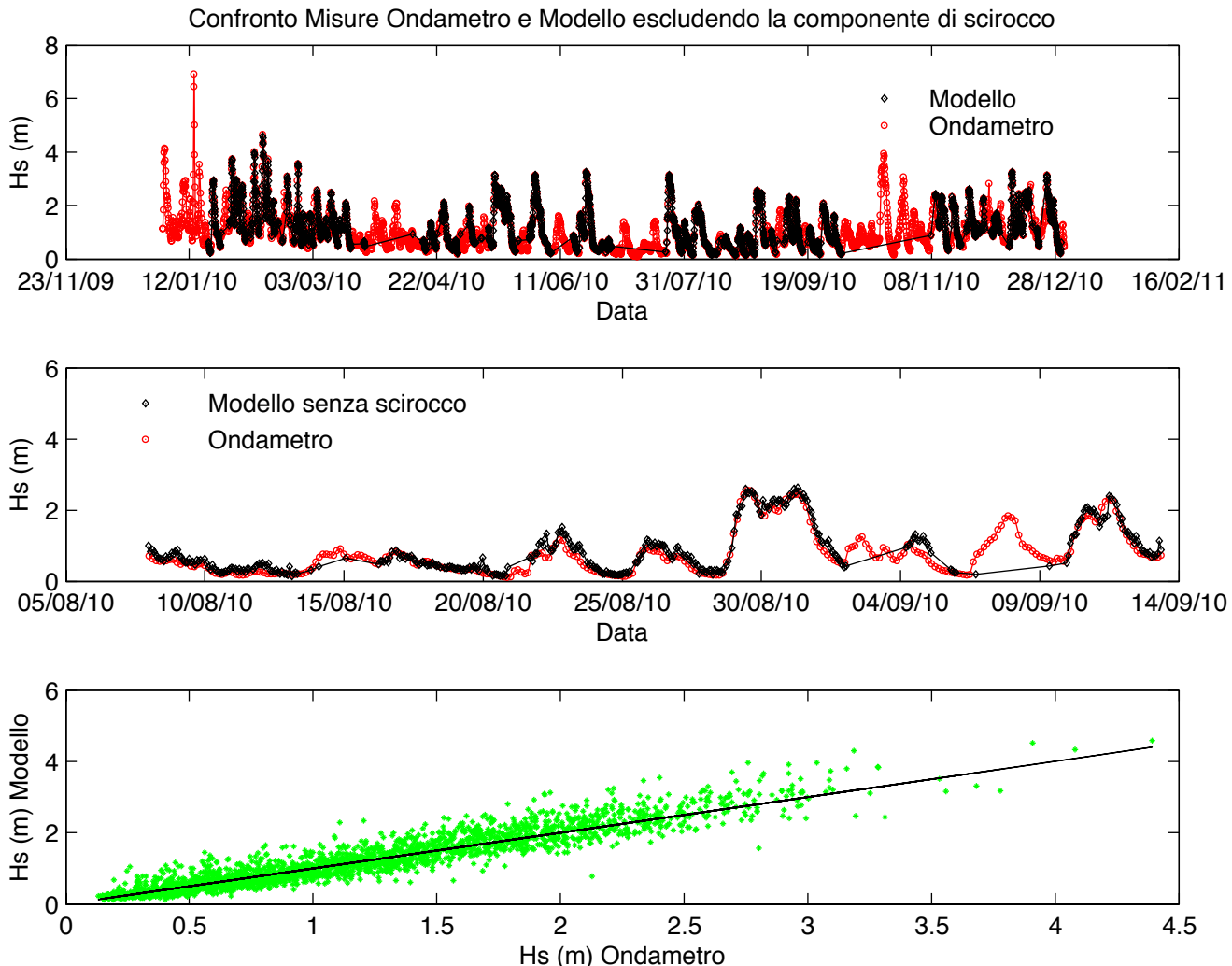
Numerical wave model validation

Numerical Wave model vs buoy: PANTELLERIA



POLITECNICO
DI TORINO

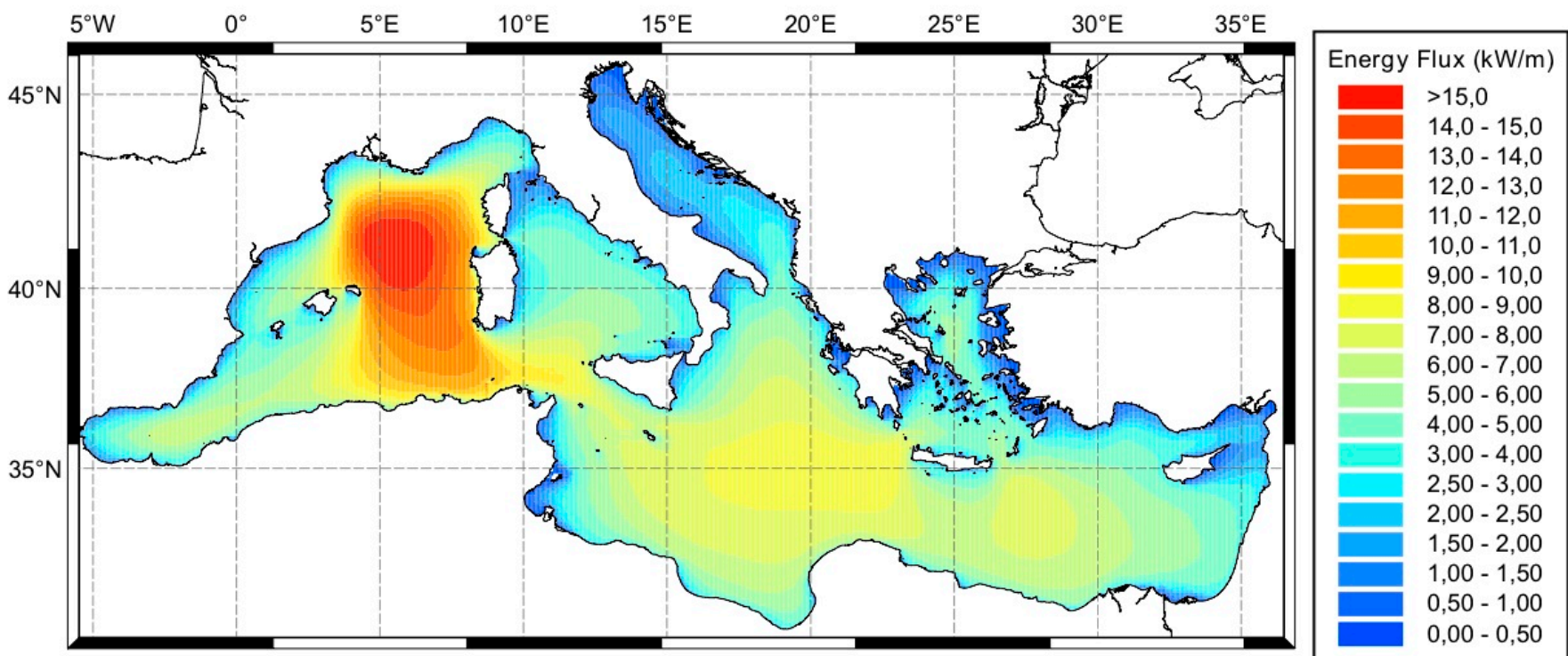
DIMEC
Dipartimento di Meccanica



Andamento delle altezze significative (Hs) in metri della simulazione SIM_ECMWF rispetto ai dati relativi alla boa di Pantelleria.

Wave energy assessment for the Mediterranean

Yearly mean climatological energy flux

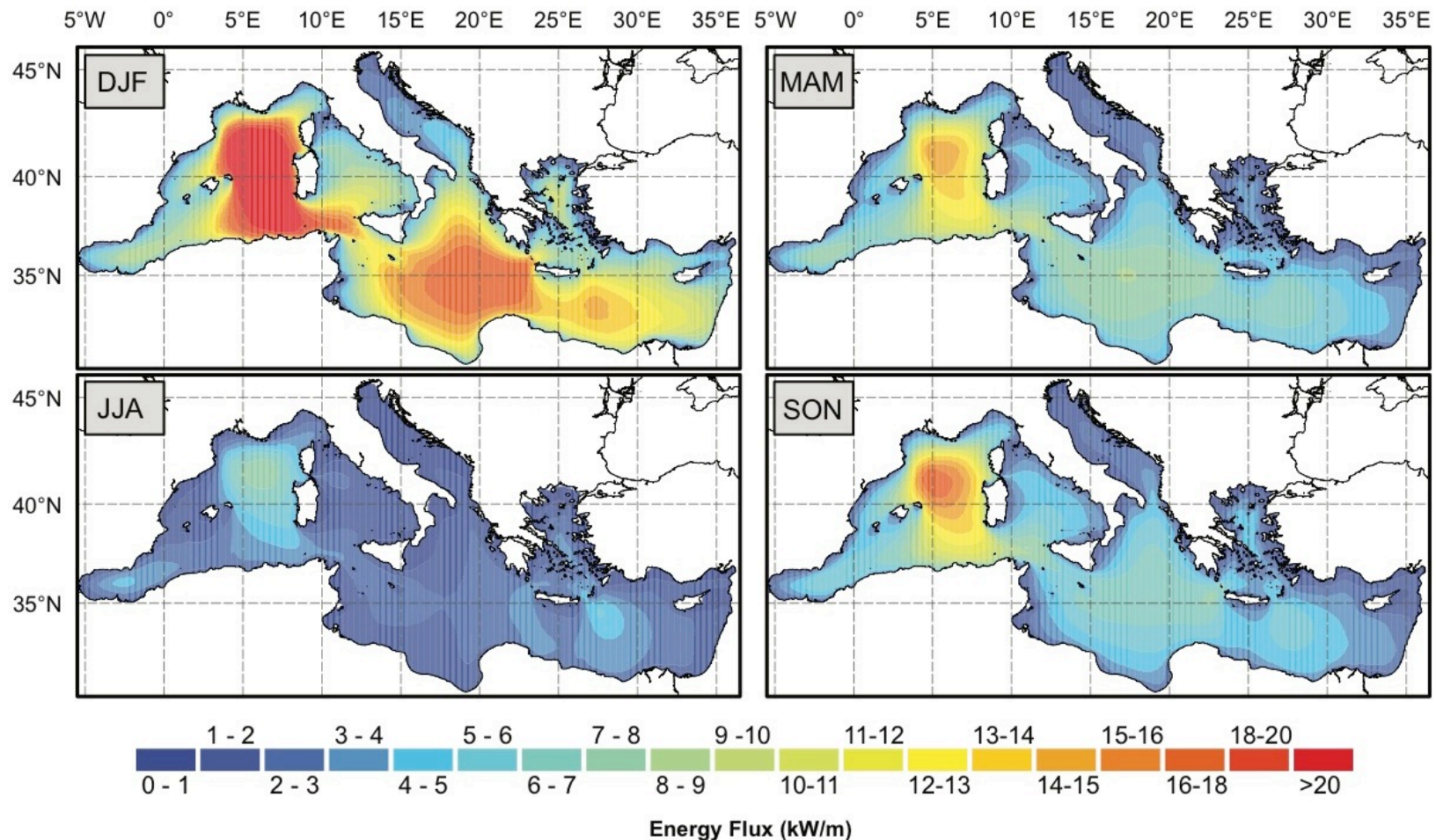


Distribution of average power per unit crest in the Mediterranean between 2001 and 2010.

$$J = \frac{\rho g^2}{64\pi} T_e H_s^2$$

Wave energy assessment for the Mediterranean

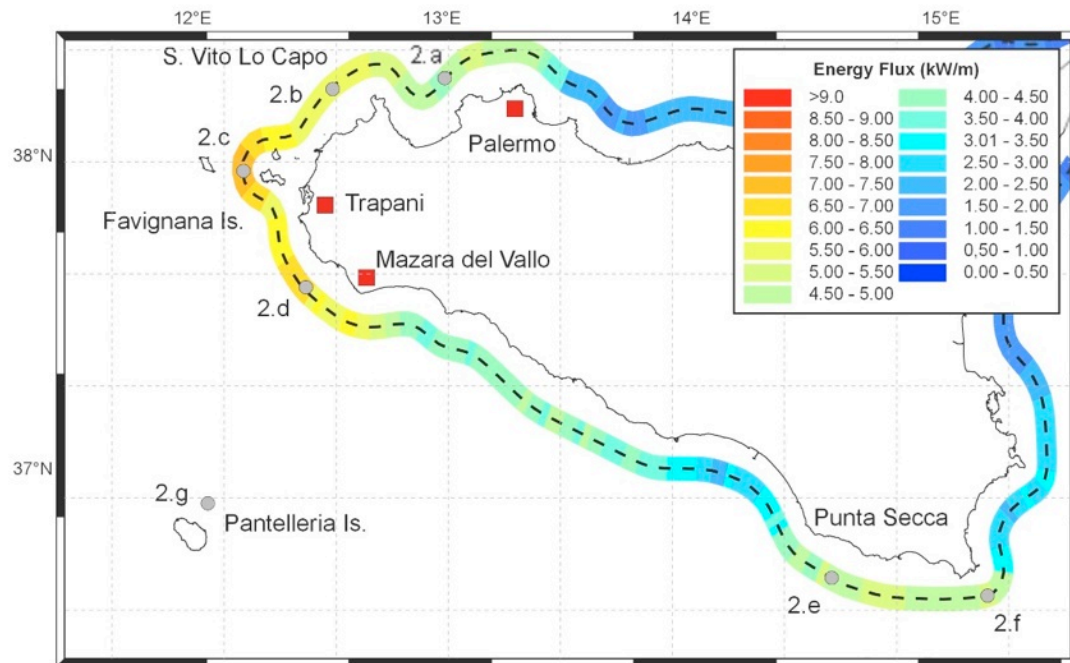
Seasonal average energy flux



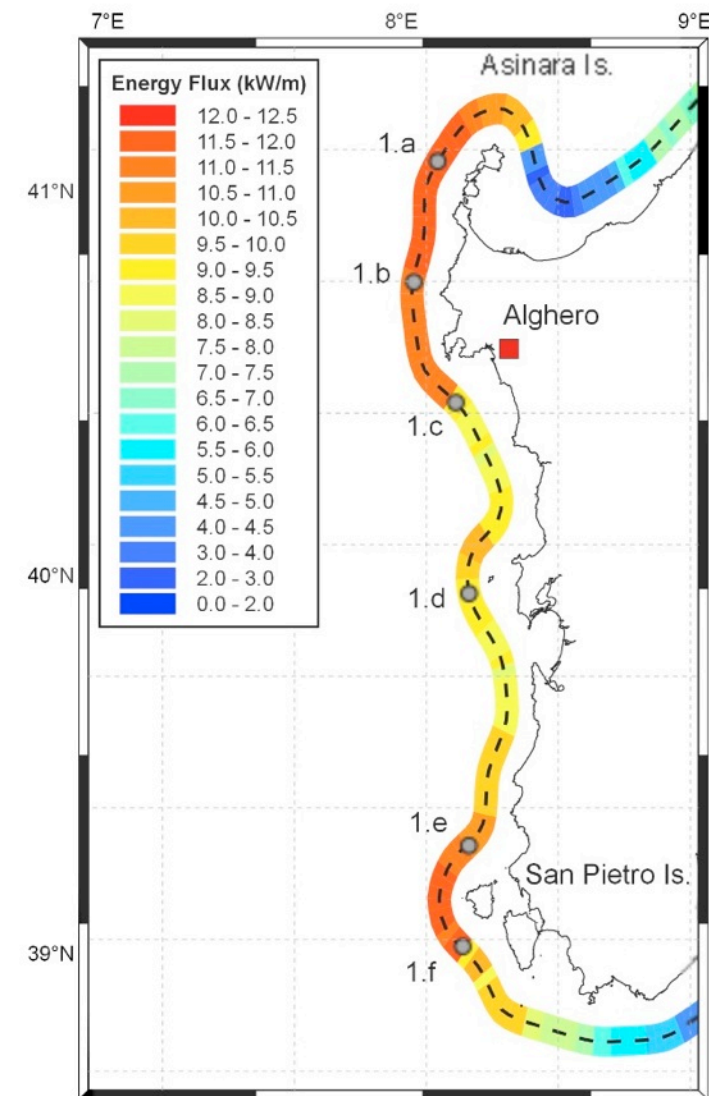
Seasonal distribution of average power per unit crest in the Mediterranean.
Averages are calculated for the entire ten years simulation.

Wave energy assessment along the Italian coasts

Distribution of average wave power flux along Sicily and west Sardinia

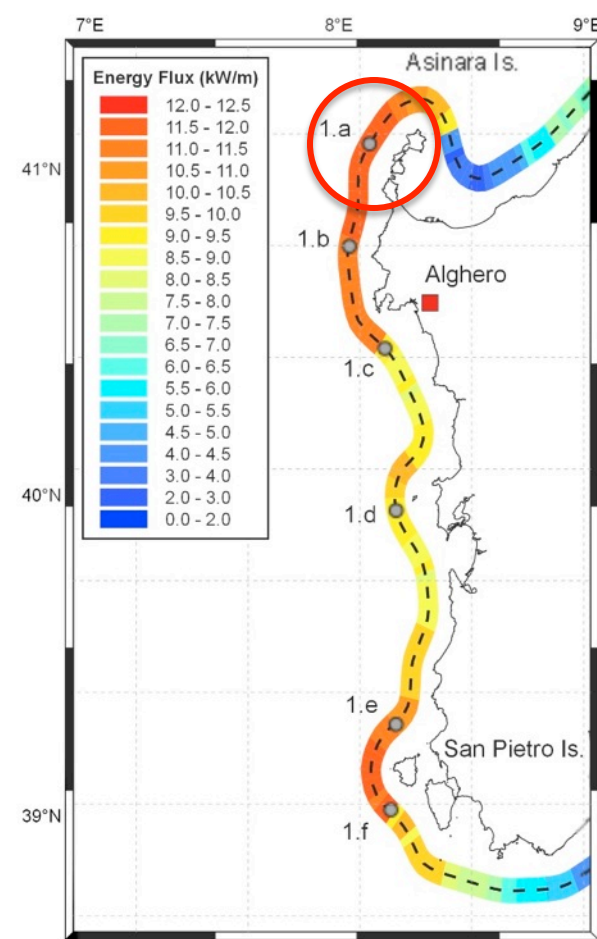
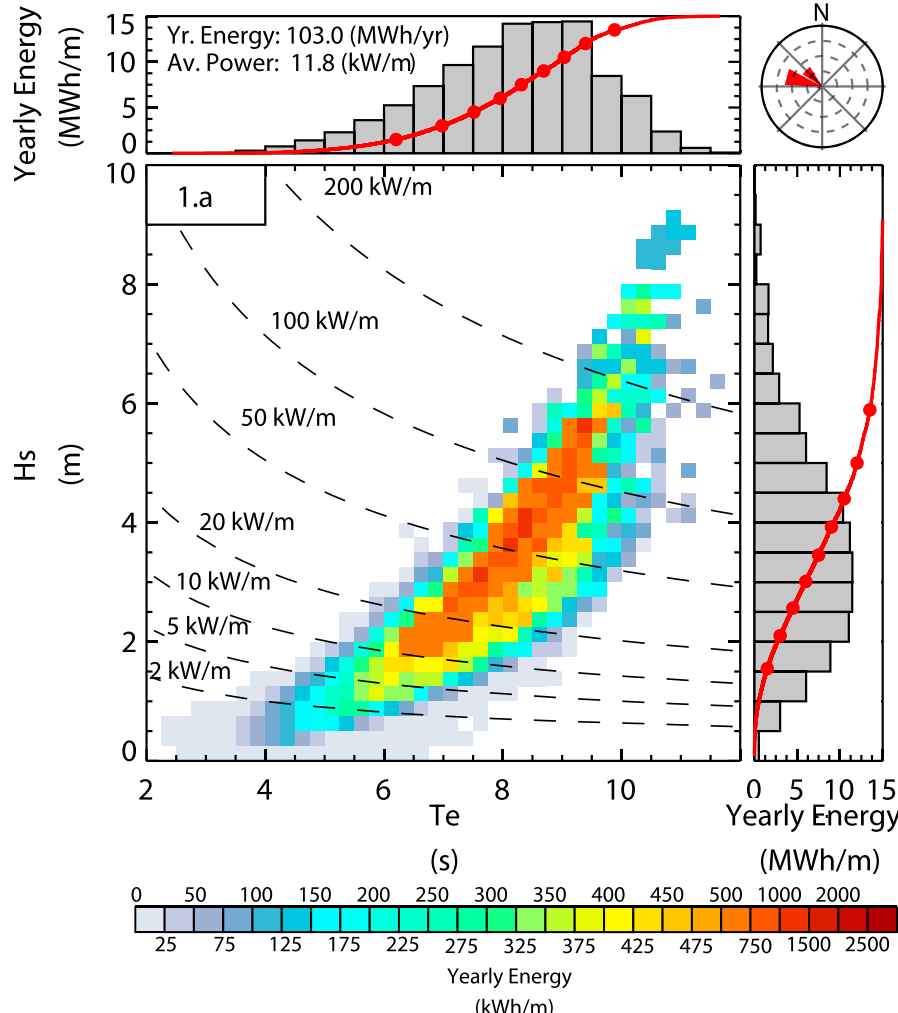


Distribution of average wave power flux per unit crest on western Sardinia and Sicilian coastline. Values are calculated on a line located 12 km off the coast.



Wave energy assessment along the Italian coasts

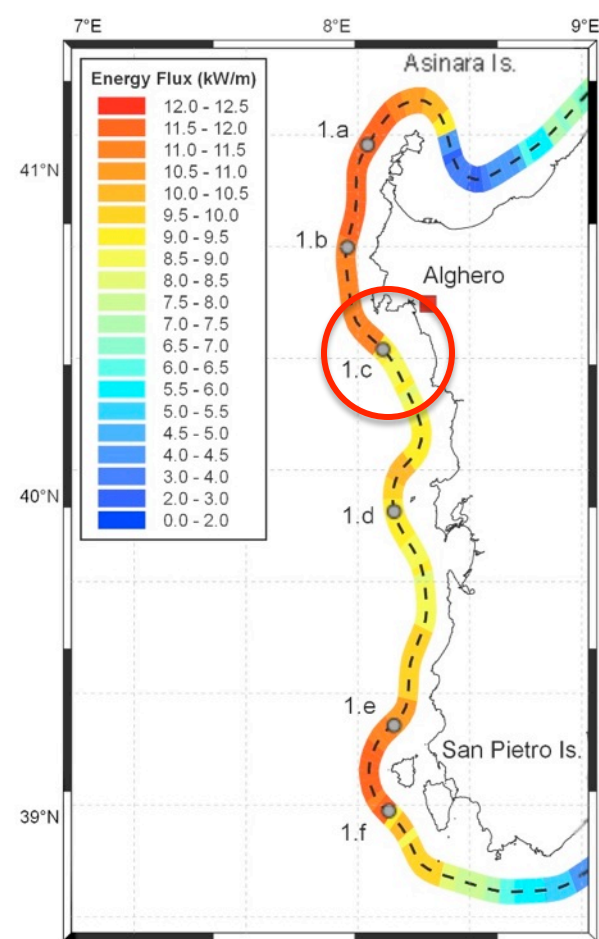
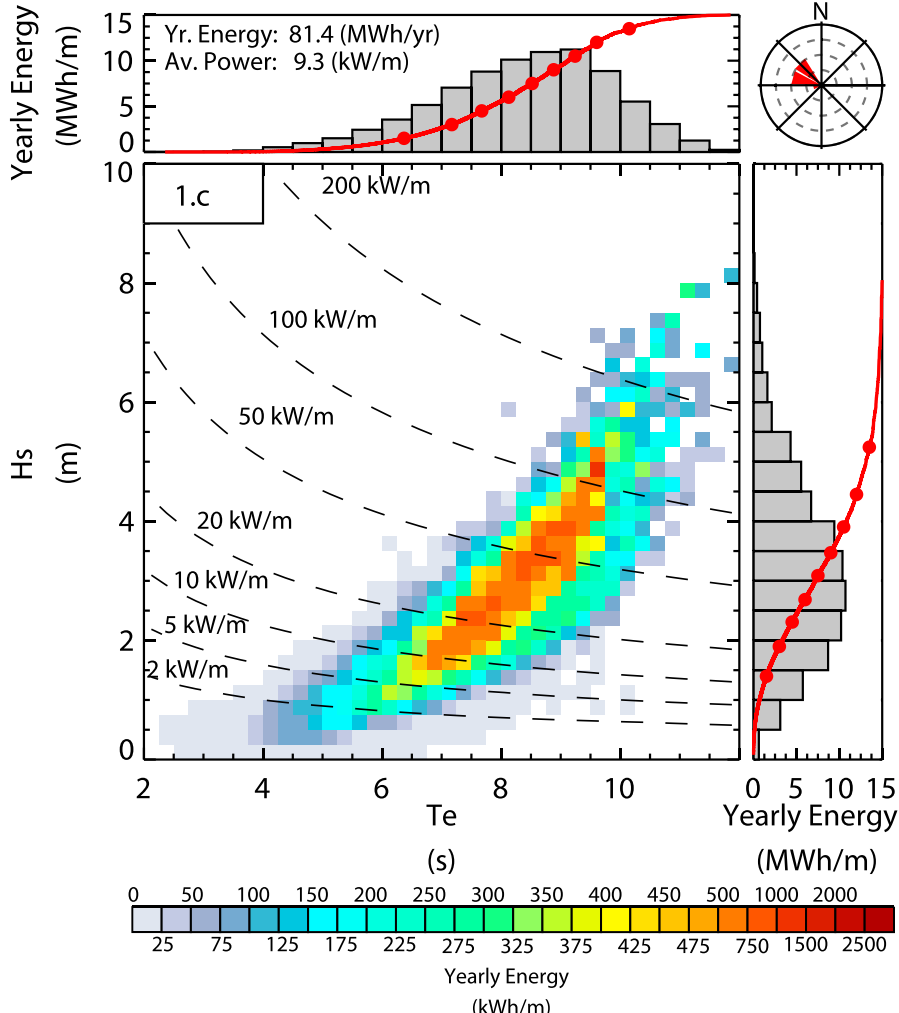
Distribution of yearly average wave energy along west Sardinia



Distribution of wave energy as a function of significant wave period and significant wave height at specific points. Lower left panel shows the average yearly energy associated with sea states identified by Te and Hs couples. Dotted lines mark reference power levels. Upper panel shows the energy distribution as a function of Te only; right panel as a function of Hs only. Red lines in the upper and right panels are the cumulative energy as a percentage of the total. Red dots on the cumulative lines mark each 10th percentile. Rose plot in the upper right panel shows energy distribution over wave incoming direction. Each circle represents 20% fractions of the total energy.

Wave energy assessment along the Italian coasts

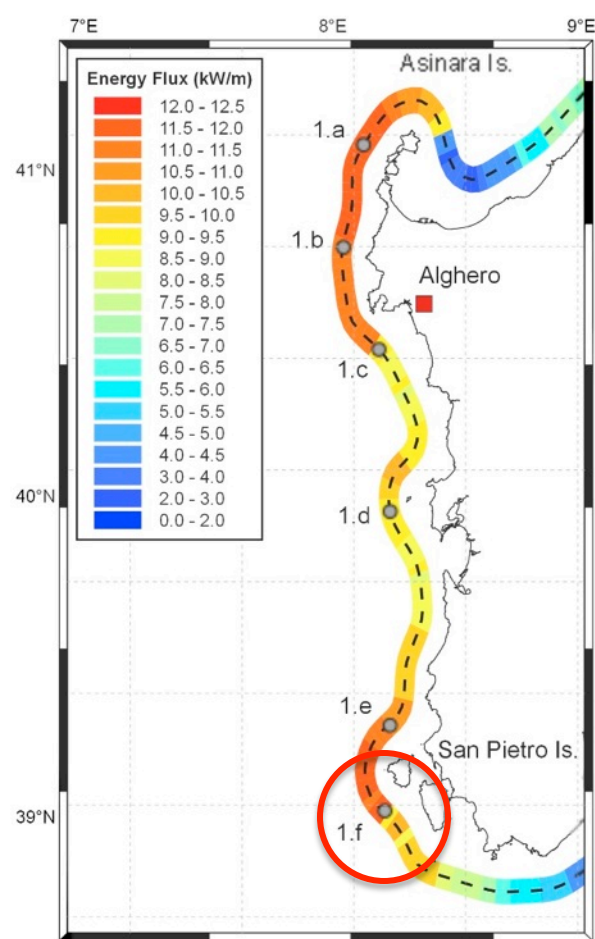
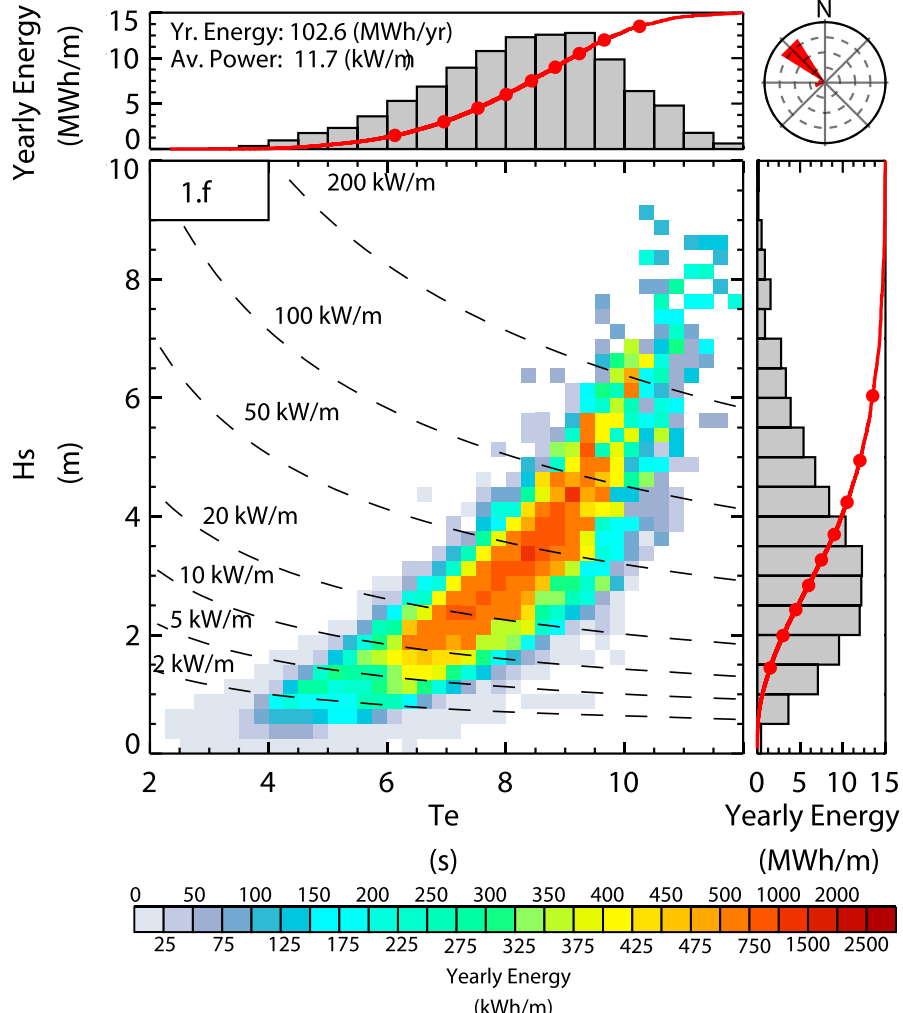
Distribution of yearly average wave energy along west Sardinia



Distribution of wave energy as a function of significant wave period and significant wave height at specific points. Lower left panel shows the average yearly energy associated with sea states identified by Te and Hs couples. Dotted lines mark reference power levels. Upper panel shows the energy distribution as a function of Te only; right panel as a function of Hs only. Red lines in the upper and right panels are the cumulative energy as a percentage of the total. Red dots on the cumulative lines mark each 10th percentile. Rose plot in the upper right panel shows energy distribution over wave incoming direction. Each circle represents 20% fractions of the total energy.

Wave energy assessment along the Italian coasts

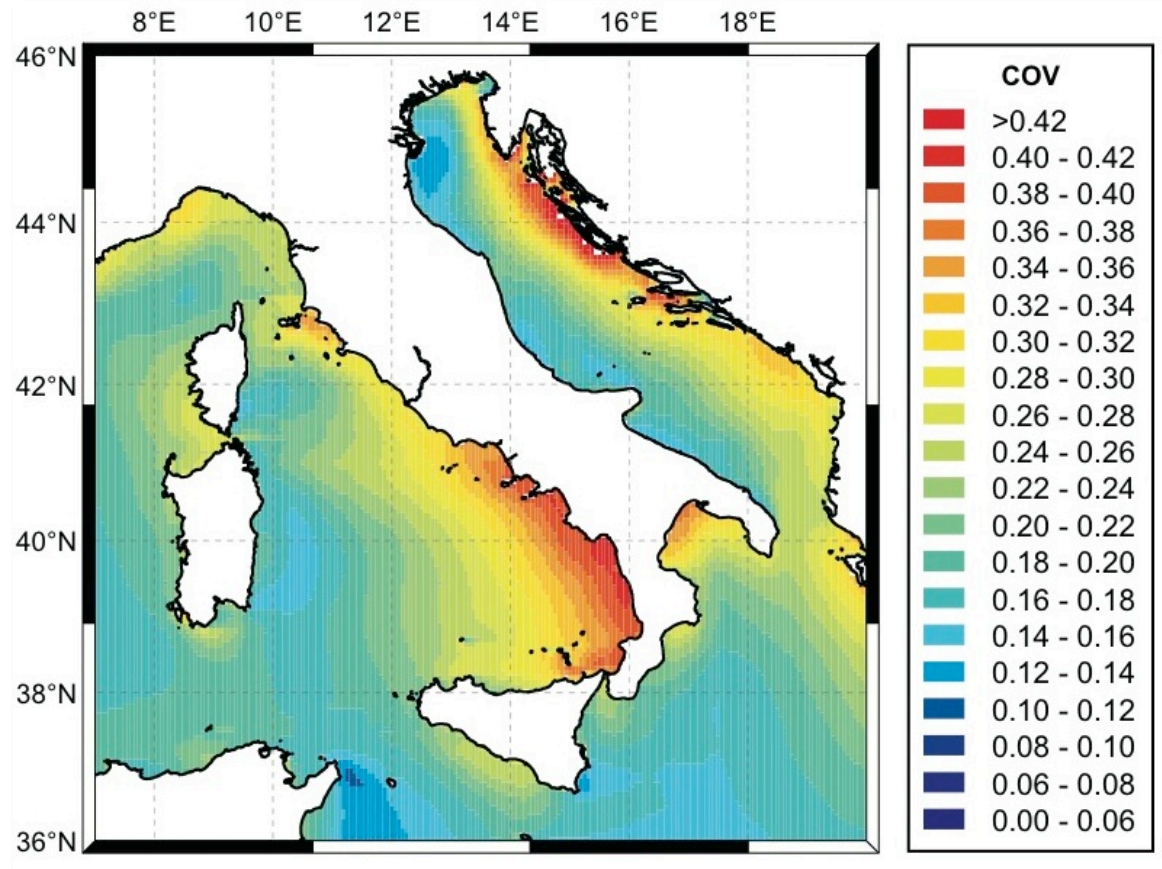
Distribution of yearly average wave energy along west Sardinia



Distribution of wave energy as a function of significant wave period and significant wave height at specific points. Lower left panel shows the average yearly energy associated with sea states identified by Te and Hs couples. Dotted lines mark reference power levels. Upper panel shows the energy distribution as a function of Te only; right panel as a function of Hs only. Red lines in the upper and right panels are the cumulative energy as a percentage of the total. Red dots on the cumulative lines mark each 10th percentile. Rose plot in the upper right panel shows energy distribution over wave incoming direction. Each circle represents 20% fractions of the total energy.

Wave energy assessment along the Italian coasts

Yearly average variability



Distribution of the Coefficient of Variation (COV) of the yearly average power fluxes for years 2001-2010 around Italy.

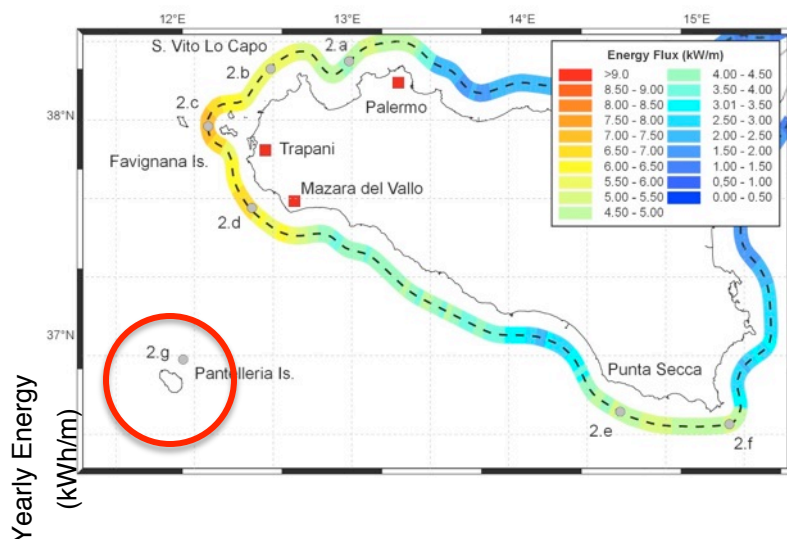
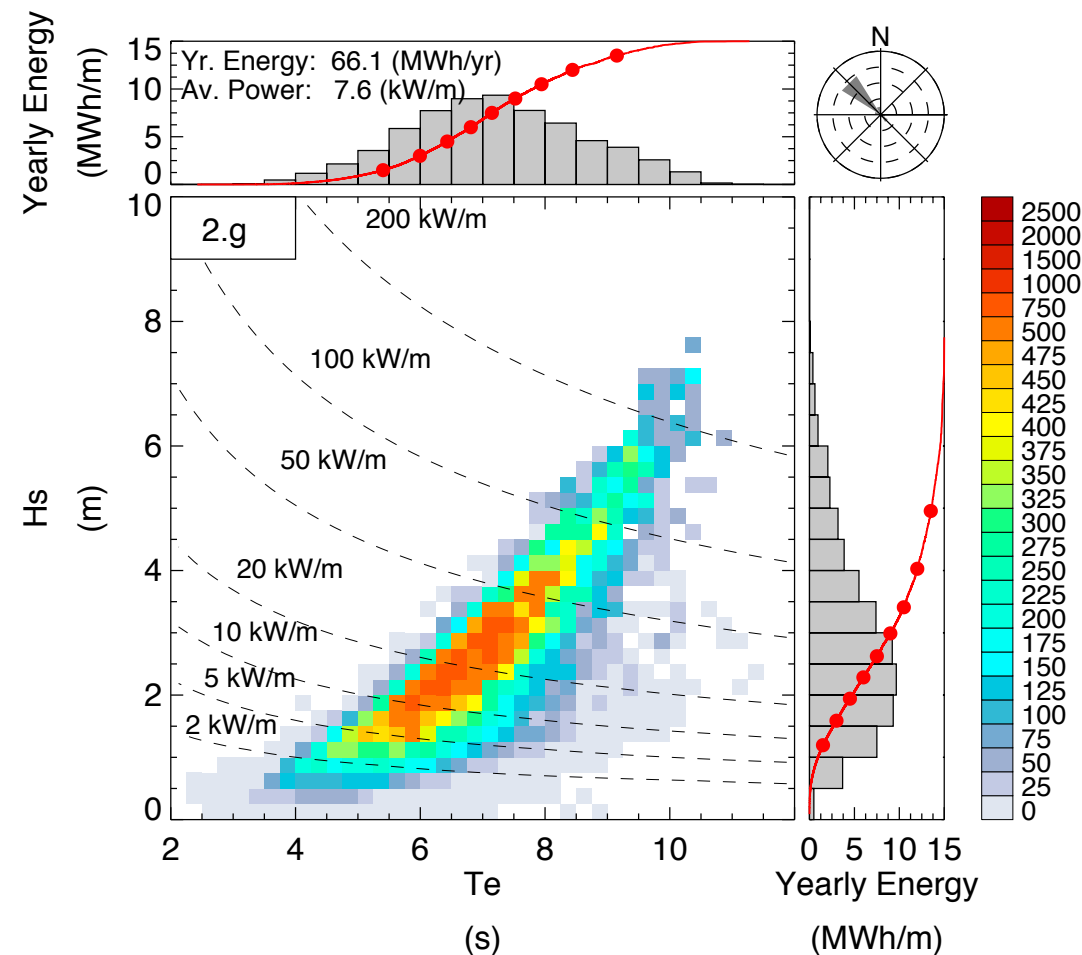
σ Standard deviation (yearly)

μ Averaged yearly value

$$COV = \frac{\sigma}{\mu}$$

Wave energy assessment along the Italian coasts

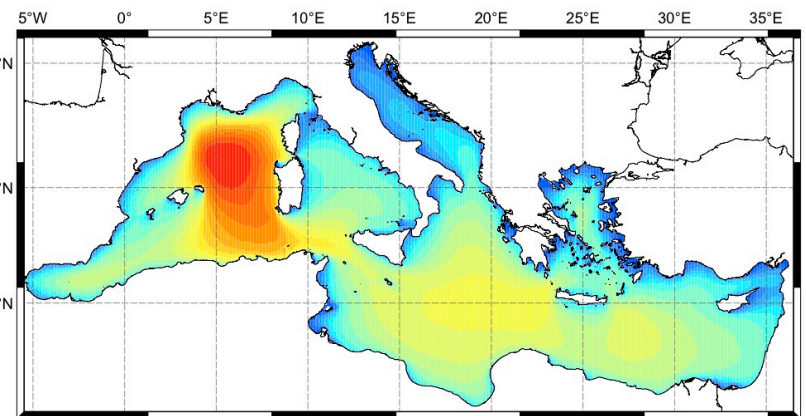
Distribution of yearly average wave energy near PANTELLERIA



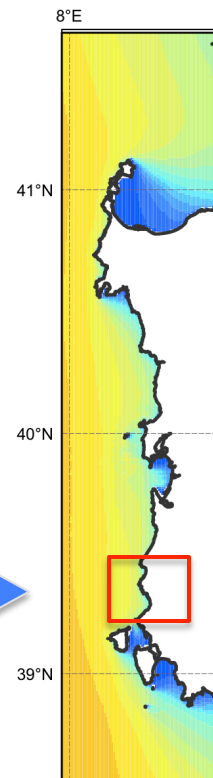
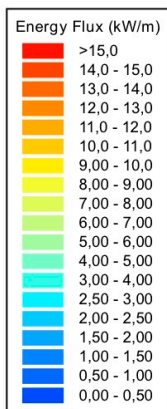
Distribution of wave energy as a function of significant wave period and significant wave height at specific points. Lower left panel shows the average yearly energy associated with sea states identified by Te and Hs couples. Dotted lines mark reference power levels. Upper panel shows the energy distribution as a function of Te only; right panel as a function of Hs only. Red lines in the upper and right panels are the cumulative energy as a percentage of the total. Red dots on the cumulative lines mark each 10th percentile. Rose plot in the upper right panel shows energy distribution over wave incoming direction. Each circle represents 20% fractions of the total energy.

High resolution numerical modeling approach

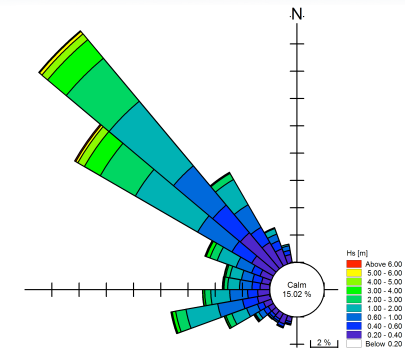
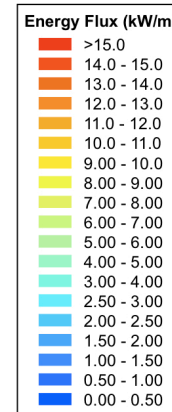
Numerical Wave model description



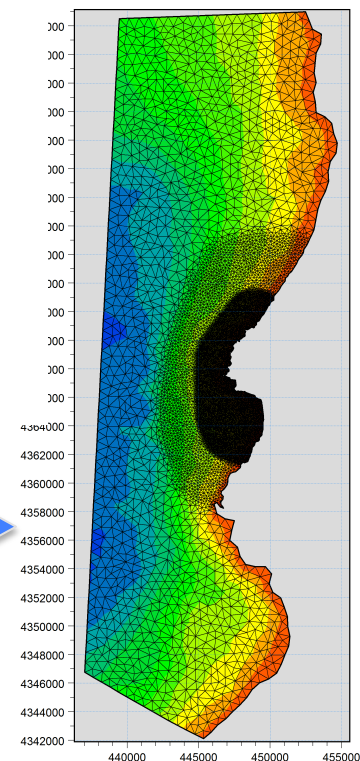
WAM
(1/16°x1/16°)



WAM/SWAN
(1/120°x120°)

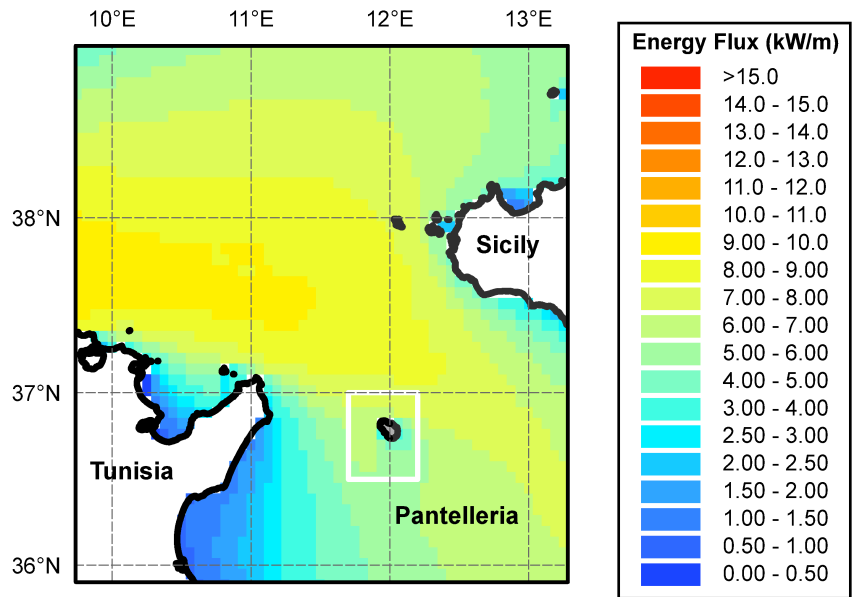


MIKE21 SW

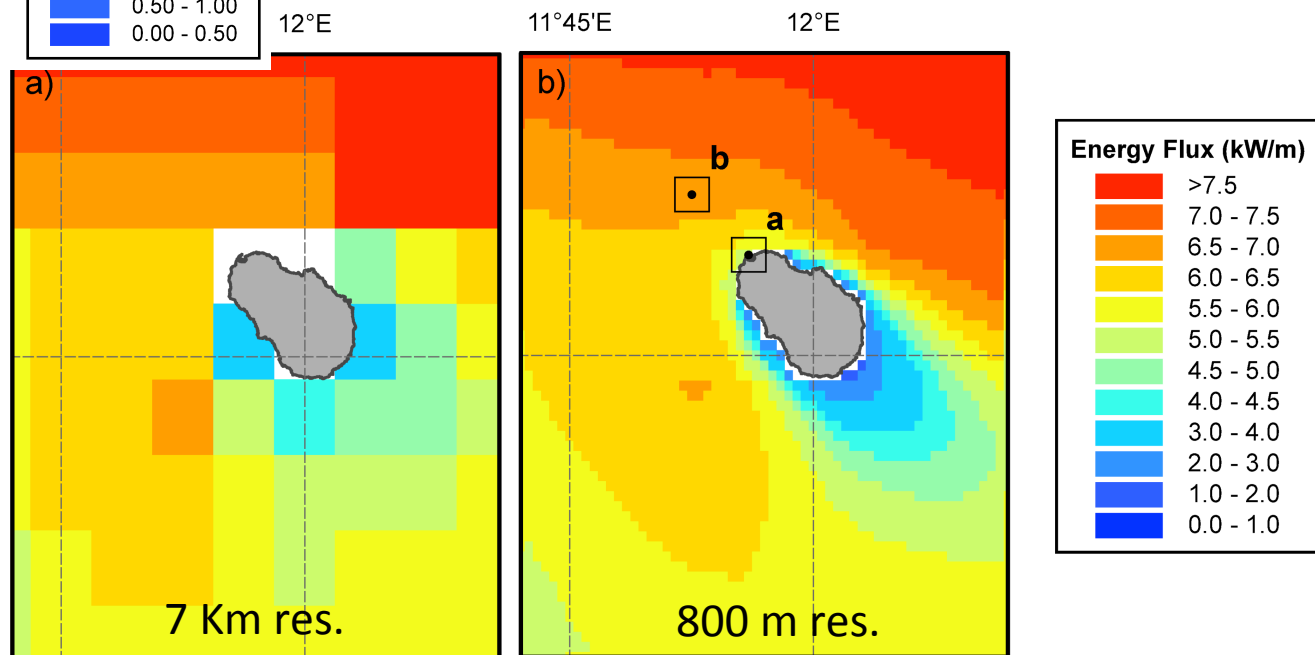


Wave energy assessment along Pantelleria island

Distribution of yearly average (2001-2010) wave energy around PANTELLERIA

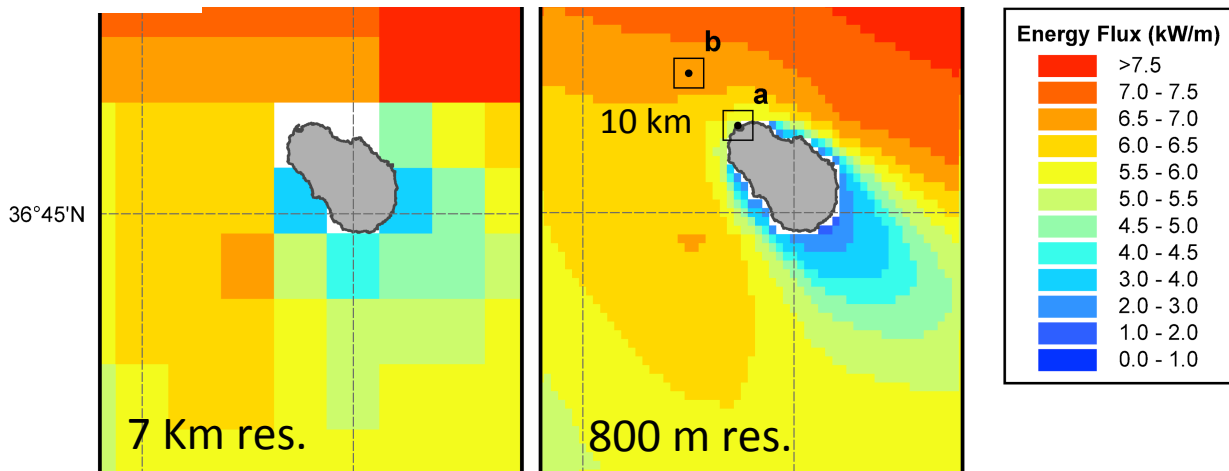
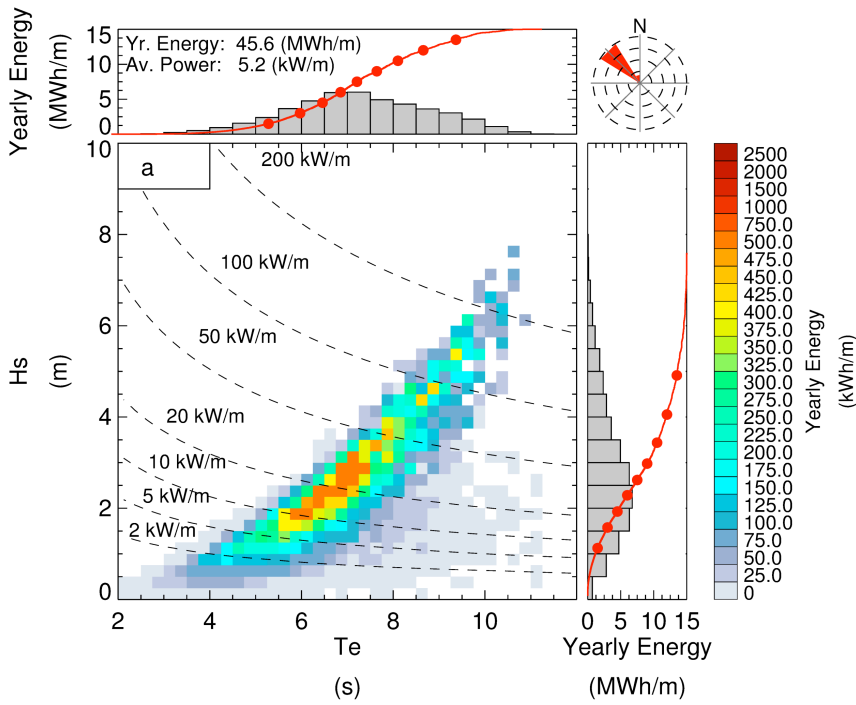
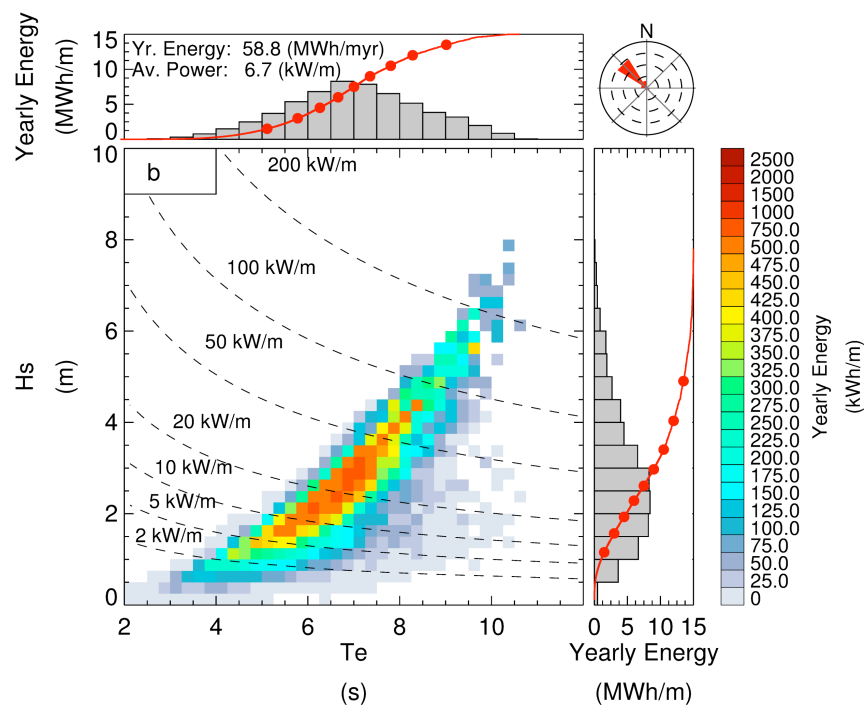


SWAN model laterally forced by the WAM simulation



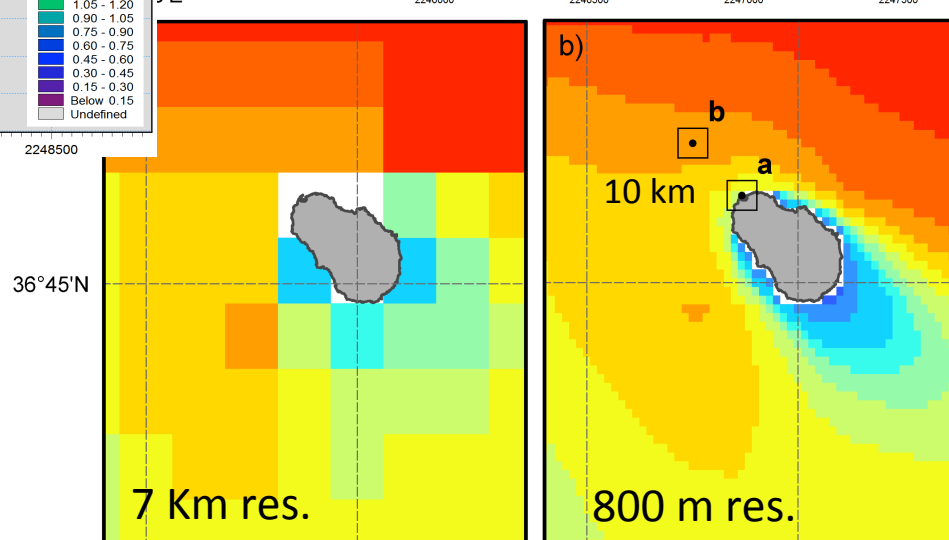
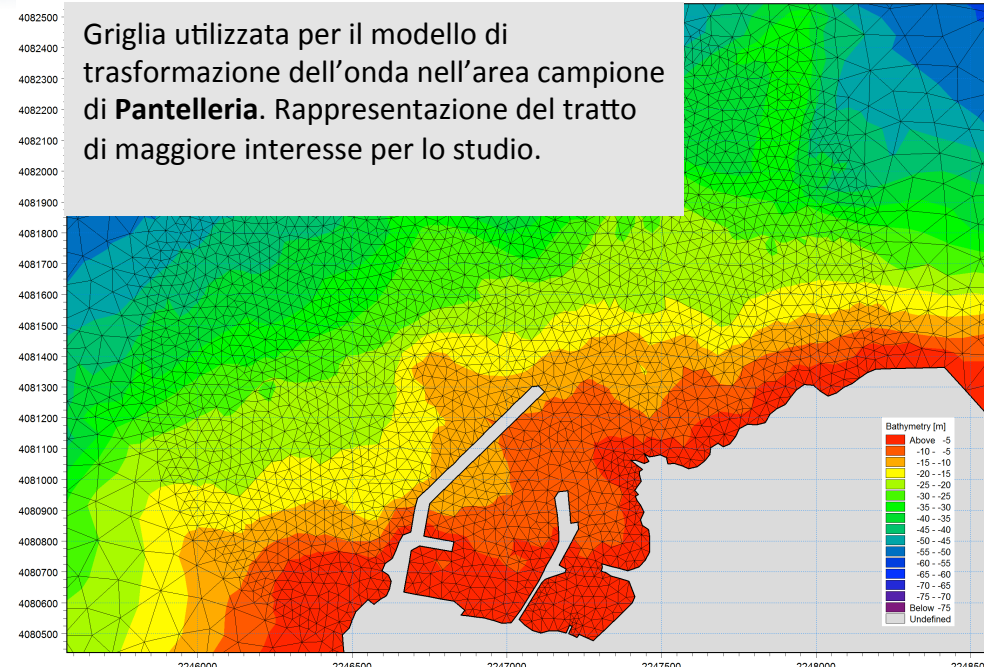
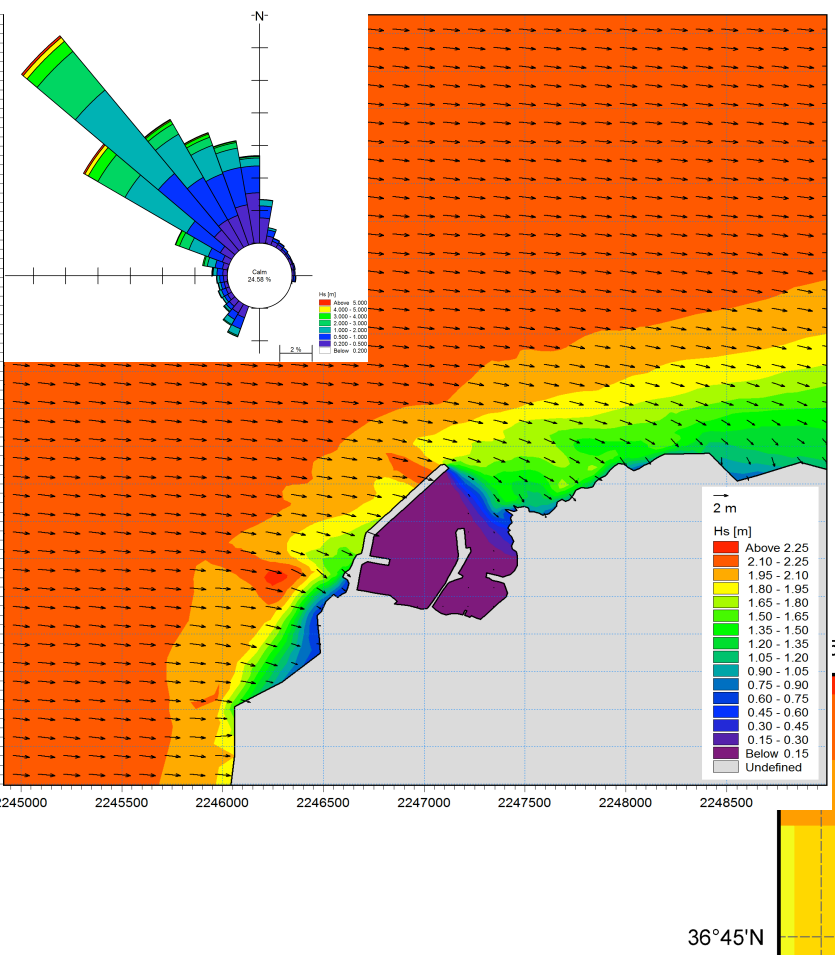
Wave energy assessment along Pantelleria island

Distribution of yearly average (2001-2010) wave energy around PANTELLERIA



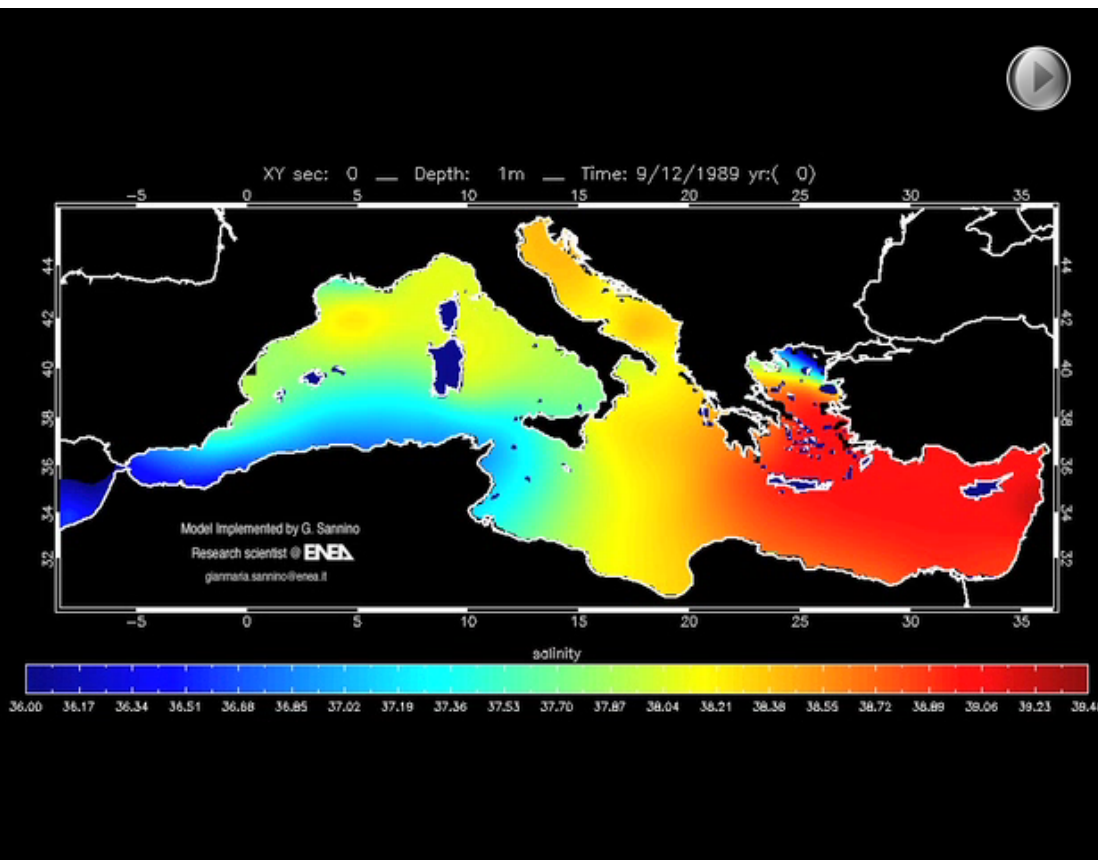
Wave energy assessment along Pantelleria island

Distribution of yearly average (2001-2010) wave energy around PANTELLERIA



Sea energy assessment - Future works

- ◆ **Using downscaled IPCC climate scenarios to asses the wave energy potential for the next future by means of the recently developed regional climate model.**



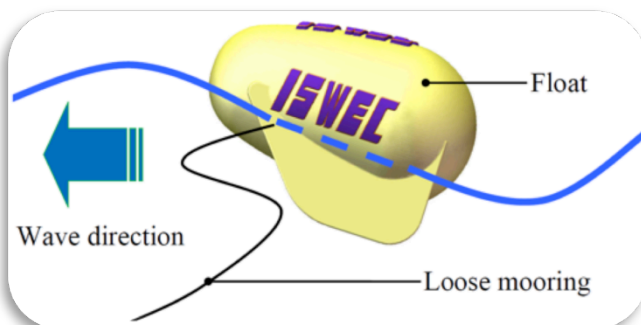
The fully coupled PROTHEUS system developed at ENEA

Sea energy assessment – Ongoing works

- ◆ **Integrating wave and tidal model results with technical data coming from recently developed Italian devices to asses the amount of electricity produced by these devices.**



UNIVERSITÀ DEGLI STUDI DI NAPOLI FEDERICO II



POLITECNICO
DI TORINO

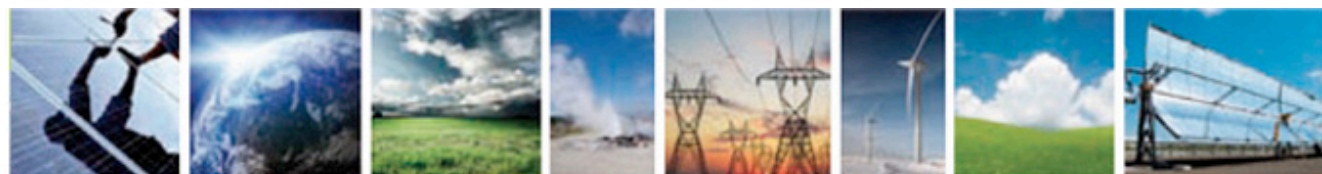
DIMEC
Dipartimento di Meccanica

European initiative

The EERA Ocean Energy JP is based around six key research themes. These themes have been developed based on existing research roadmaps which identify the critical areas of research required for the successful growth of the industry. The Research Themes are here:

- Resource
- Devices and Technology
- Deployment and Operations
- Environmental Impact
- Socio-economic Impact
- Research Infrastructure, Education and Training

Within each Research Theme a number of sub-topics have been identified as key long term research objectives. Initial EERA Ocean Energy JP activities are not able to cover all of the objectives identified but have been prioritized in the first year's programme by need and the current availability of funding. The gap between what has been identified as a key long term objective and what the EERA Ocean Energy JP is actually able to deliver in the first year will help identify issues that need future funding and coordinated research efforts.



www.eera-set.eu

**Coordinating energy research
for a low Carbon Europe**



Some References

- Liberti L., A. Carillo, G. Sannino, (2012): Wave energy resource assessment in the Mediterranean, the Italian perspective.. Renewable Energy 2012
- Sanchez-Garrido, J. C., G. Sannino, L. Liberti, J. Garcia Lafuente, and L. J. Pratt (2011): Numerical modelling of three-dimensional stratified tidal flow over Camarinal Sill, Strait of Gibraltar. *J. Geophys. Res.*, VOL. 116, C12026, doi:10.1029/2011JC007093.
- Sannino G., L. Liberti, A. Carillo, A. Bargagli, E. Caiaffa (2011): Prospettive di sviluppo dell'energia dal mare per la produzione elettrica in Italia. *Energia, Ambiente e Innovazione -Rivista ENEA* - n. 4-5/2011.
- Sannino G., A. Bargagli, A. Carillo, E. Caiaffa, E. Lombardi, P. Monti, G. Leuzzi (2011): Valutazione del potenziale energetico del moto ondoso lungo le coste italiane. Report RdS/2011/151.
- Bargagli A. , A. Carillo, V. Ruggiero, P. Lanucara, G. Sannino (2011): Modello di onde per l'area mediterranea. Report RdS/2011/26.
- Carillo A., E. Napolitano, G. Leuzzi, P. Monti, P. Lanucara, V. Ruggiero, G. Sannino: (2011): Valutazione del potenziale energetico delle correnti marine del Mar Mediterraneo. Report RdS/2011/65.
- Protheus Group (Sannino is included) (2009), An atmosphere–ocean regional climate model for the Mediterranean area: assessment of a present climate simulation. *Climate Dynamics*, DOI 10.1007/s00382-009-0691-8
- Sannino G., Herrmann M., Carillo A., Rupolo V., Ruggiero V., Artale V. Heimbach P. (2009), An eddy-permitting model of the Mediterranean Sea with a two-way grid refinement at the Strait of Gibraltar. *Ocean Modelling*, Vol 30, 1, 56-72. DOI: 10.1016/j.ocemod.2009.06.002
- Sannino G., L. Pratt and A. Carillo (2009), Hydraulic criticality of the exchange flow through the Strait of Gibraltar, *J. of Physical Oceanography*, Vol 39, 11, 2779-2799. DOI: 10.1175/2009JPO4075.1
- Sannino G., A. Bargagli and V. Artale (2004), Numerical modeling of the semidiurnal tidal exchange through the Strait of Gibraltar, *Journal of Geophysical Research*, Vol. 109, C05011, doi:10.1029/2003JC002057.